Volume 42, Number 1, 2016.

Mobility & Vehicle Mechanics

International Journal for Vehicle Mechanics, Engines and Transportation Systems

ISSN 1450 - 5304

UDC 621 + 629(05)=802.0

UNIVERSITY OF KRAGUJEVAC, FACULTY OF ENGINEERING

SERBIAN SOCIETY OF AUTOMOTIVE ENGINEERS

M V M **M**obility **V**ehicle **M**echanics

*Editors: Prof. dr **Jovanka Lukić**; Prof. dr **Čedomir Duboka***

MVM *Editorial Board*
University of Kragujevac
Faculty of Engineering
Sestre Janjić 6, 34000 Kragujevac, Serbia
Tel.: +381/34/335990; Fax: + 381/34/333192

Prof. Dr **Belingardi Giovanni**
Politecnico di Torino,
Torino, ITALY

Dr Ing**. Ćućuz Stojan**
Visteon corporation,
Novi Jicin,
CZECH REPUBLIC

Prof. Dr **Demić Miroslav**
University of Kragujevac
Faculty of Engineering
Kragujevac, SERBIA

Prof. Dr **Fiala Ernest**
Wien, OESTERREICH

Prof. Dr **Gillespie D. Thomas**
University of Michigan,
Ann Arbor, Michigan, USA

Prof. Dr **Grujović Aleksandar**
University of Kragujevac
Faculty of Engineering
Kragujevac, SERBIA

Prof. Dr **Knapezyk Josef**
Politechniki Krakowskiej,
Krakow, POLAND

Prof. Dr **Krstić Božidar**
University of Kragujevac
Faculty of Engineering
Kragujevac, SERBIA

Prof. Dr **Mariotti G. Virzi**
Universita degli Studidi Palermo,
Dipartimento di Meccanica ed
Aeronautica,
Palermo, ITALY

Prof. Dr **Pešić Radivoje**
University of Kragujevac
Faculty of Engineering
Kragujevac, SERBIA

Prof. Dr **Petrović Stojan**
Faculty of Mech. Eng. Belgrade,
SERBIA

Prof. Dr **Radonjić Dragoljub**
University of Kragujevac
Faculty of Engineering
Kragujevac, SERBIA

Prof. Dr **Radonjić Rajko**
University of Kragujevac
Faculty of Engineering
Kragujevac, SERBIA

Prof. Dr **Spentzas Constatinos**
N. National Technical University,
GREECE

Prof. Dr **Todorović Jovan**
Faculty of Mech. Eng. Belgrade,
SERBIA

Prof. Dr **Toliskyj Vladimir E.**
Academician NAMI,
Moscow, RUSSIA

Prof. Dr **Teodorović Dušan**
Faculty of Traffic and Transport
Engineering,
Belgrade, SERBIA

Prof. Dr **Veinović Stevan**
University of Kragujevac
Faculty of Engineering
Kragujevac, SERBIA

For Publisher: Prof. dr Miroslav Živković, dean, University of Kragujevac, Faculty of Engineering

Publishing of this Journal is financially supported from:
Ministry of Education, Science and Technological Development, Republic Serbia

Mobility & **V**ehicle **M**echanics

Motorna **V**ozila i **M**otori

Volume 42
Number 1
2016.

Mobility & **V**ehicle **M**echanics

Motorna **V**ozila i **M**otori

Volume 42
Number 1
2016.

INFLUENCE OF WORKING REGIMES ON DOUBLE VIBE FUNCTION PARAMETERS FOR DIESEL ENGINES

Ivan Grujić[1]*, Aleksandar Davinić*

UDC: 621.436:621.43.016

ABSTRACT: No mathematical model can replace the experiment. However, because it saves time and money are often approached mathematical models that sufficiently describe a process. Double Vibe function is used to describe the combustion process in diesel engines with direct injection. Double Vibe function parameters are determined on the basis of measured data of 13 working regimes on a mono-cylindrical engine in the Laboratory for IC engines at the Faculty of engineering in Kragujevac. With this method is not possible to define all parameters, because small number of working regimes.

KEY WORDS: mathematical model, double Vibe function, diesel engine.

UTICAJ RADNIH REŽIMA NA PARAMETRE DVOSTEPENE VIBE FUNKCIJE KOD DIZEL MOTORA

REZIME: Nijedan matematički model ne može zameniti eksperiment. Međutim zbog uštede vremena i novca često se pristupa matematičkim modelima koji u dovoljnoj meri opisuju neki proces. Dvostepena Vibe funkcija se koristi za opisivanje procesa sagorevanja kod dizel motora sa direktnim ubrizgavanjem. Parametri dvostepene Vibe funkcije su određeni na osnovu podataka od 13 radnih režima izmerenih na monocilindričnom motoru u Laboratoriji za motore SUS na Fakultetu inženjerskih nauka u Kragujevcu. Ovom metodom nije moguće definisati sve parametre, zbog malog broja radnih režima.

KLJUČNE REČI: matematički model, dvostepena Vibe funkcija, dizel motor.

[1] *Received October 2015, Revised November 2015, Published On Line December 2015*

Intentionally blank

INFLUENCE OF WORKING REGIMES ON DOUBLE VIBE FUNCTION PARAMETERS FOR DIESEL ENGINES

Ivan Grujić[1], Ph. D Student, Aleksandar Davinić[2], Ph. D, Assistant professor

UDC:621.436:621.43.016

INTRODUCTION

More the one century in vehicle are dominating two basic groups of engines:

- petrol engines, and
- diesel engines.

Diesel engine is always considered to be more economical. Therefore it can be said that the diesel engine is widely used in today's vehicles.

From the time of inception to the present day, the diesel engine is largely changed, and always will exist in the future need to develop new and improving existing engines.

When developing new and improving existing engines, it is necessary to do many studies, including the study about combustion process in engine cylinder. Off course indispensable part of every research is experiment. However, the performance of the experiment requires equipment and time. Specifically, the performance of the experiment can be very expensive and long. Today are very often used mathematical models. The main reason for the growth in engine modelling activities arises from the economic benefits; by using computer models, large savings are possible in expensive experimental work when engine modifications are being considered. Models cannot replace real engine testing but they are able to provide good estimates of performance changes resulting from possible engine modifications and thus can help in selecting the best options for further development, reducing the amount of hardware development required [1]. In this paper is described the methodology of modelling combustion process, with purpose to see how the working regimes affect on double Vibe parameters.

One of the most famous equations or functions that are used for modelling the combustion process in IC engines is Vibe function. Author of function is Ivan Ivanovitch Wiebe (1902-1969) [2].

1. COMBUSTION PROCESS MODELING BY DOUBLE VIBE FUNCTION

The Vibe function is often used to approximate the actual heat release characteristics of an engine:

$$\frac{dx}{d\left(\frac{\phi}{\phi_z}\right)} = \frac{a}{\phi_z}(m+1)\left(\frac{\phi}{\phi_z}\right)e^{-a\left(\phi/\phi_z\right)^{m+1}} \tag{1}$$

[1] *Ivan Grujić, University of Kragujevac, Faculty of Engineering, Sestre Janjić 6, 34000 Kragujevac, email:ivagrujićdd@gmail.com*

[2] *Aleksandar Davinić, University of Kragujevac, Faculty of Engineering, Sestre Janjić 6, 34000 Kragujevac, email: davinic@kg.ac.rs*

The integral of the Vibe function gives the fraction of the fuel mass that has been burned since the start of combustion:

$$x = 1 - e^{-a\left(\phi/\phi_z\right)^{m+1}} \tag{2}$$

$$x_1 = \sigma_g \cdot x = \sigma_g \cdot \left[1 - e^{-a\left(\phi_1/\phi_{z1}\right)^{m_1+1}}\right]$$
$$\frac{dx_1}{d\left(\frac{\phi_1}{\phi_{z1}}\right)} = \sigma g \cdot \frac{a}{\phi_{z1}}\left(m_1+1\right)\left(\frac{\phi_1}{\phi_{z1}}\right)e^{-a\left(\phi_1/\phi_{z1}\right)^{m_1+1}} \tag{3}$$

For modelling combustion process in diesel engines with direct injection is used double Vibe function. Relations (3) are used to describe the first part of the double Vibe function, and relations (4) to describe the second part.

$$x_2 = \left(1-\sigma_g\right)\cdot x = \left(1-\sigma_g\right)\cdot\left[1 - e^{-a\left(\phi_2/\phi_{z2}\right)^{m_2+1}}\right]$$
$$\frac{dx_2}{d\left(\frac{\phi_2}{\phi_{z2}}\right)} = \left(1-\sigma_g\right)\cdot\frac{a}{\phi_{z2}}\left(m_2+1\right)\left(\frac{\phi_2}{\phi_{z2}}\right)e^{-a\left(\phi_2/\phi_{z2}\right)^{m_2+1}} \tag{4}$$

Double Vibe function is expressed as the sum of the first and second part of the Vibe function:

$$x = x_1 + x_2$$
$$\frac{dx}{d\varphi} = \frac{dx_1}{d\varphi} + \frac{dx_2}{d\varphi} \tag{5}$$

where:

- x - is cumulative normalized heat released (mass fraction burned),
- ϕ - is angle between initial and current time of the simple Vibe function,
- ϕ_z - is duration angle of the simple Vibe function (duration of the heat release),
- m - is Vibe function shape parameter,
- a - is Vibe function parameter, $a = 6.908$, and
- σ_g - is the share of fuel mass burnt as describe by the first Vibe function.

The appearance of a double Vibe function is shown in Figure 1.

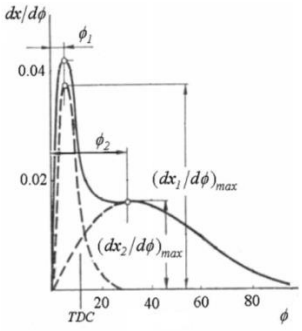

Figure 1 Double Vibe function [2]

2. EXPERIMENTAL RESARCH

One of the most frequently used ways to obtain necessary information about the working process is recording of the cylinder pressure. Even without any calculation, the cylinder pressure record provides some information about combustion in engine cylinder, for example: peak pressure and its position, the rate of pressure rise… Information can be obtained by analysing indicator diagram.

Pressure recording was performed in the Laboratory for IC engines of the Faculty of Engineering in Kragujevac. Test engine is shown on Figure 2, and measuring chain used for measurement of cylinder pressure on Figure 3.

Figure 2 Test engine

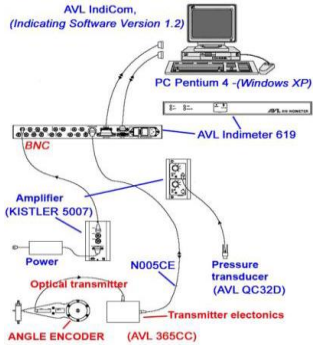

Figure 3 AVL Indicating system diagram [1]

The 450 was used in experiment. It is mono-cylindrical, air-cooled DI-diesel engine. Compression ratio of this engine is 17.5. Injection timing was fixed at 18.5 °CA at all regimes. Engine is loaded by hydraulic brake, SCHENK U116/2, Figure 4.

Figure 4 Engine brake SCHENK U116/2

Recording pressure was performed on 13 working regimes (Figure 5), and for every regime was obtained indicator diagram (Figure 6).

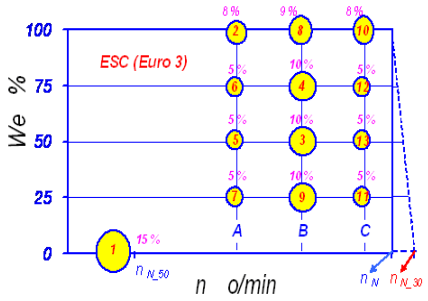

Figure 5 Working regimes [4]

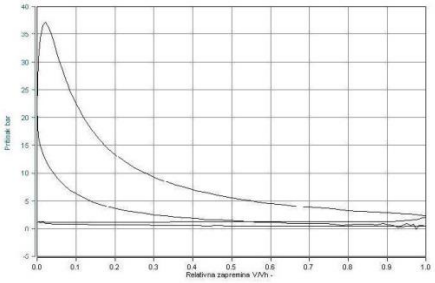

Figure 6 Indicator diagram for one of the regimes

Based on the data of pressure values that are obtained from the indicator diagrams for each working regime is modelled combustion law using Vibe function, and using software are obtained values for Vibe function parameters.

3. INFLUENCE OF WORKING REGIMES ON DOUBLE VIBE FUNCTION PARAMETERS

Figure 7 shows the influence of engine speed and engine load on the first Vibe function shape parameter. It may be concluded that engine load and engine speed do not have significant influence on the first Vibe function shape parameter. The smallest value of the first Vibe function shape parameter is recorded at $n = 2687$ rpm and highest value at $n = 2325$ rpm.

Figure 8 shows the influence of engine speed and engine load on the second Vibe function shape parameter. In this case, the second Vibe function shape parameter have the biggest values on the smallest values of the engine load and conversely.

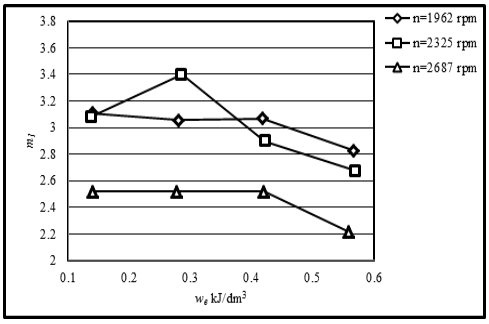

Figure 7 Influence of working regimes on the first Vibe function shape parameter

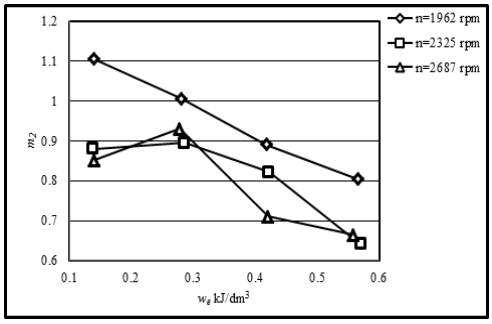

Figure 8 Influence of working regimes on the second Vibe function shape parameter

$$n = 1962 \text{ rpm} \qquad m_1 = -2{,}335 \cdot w_e^2 + 1{,}0584 \cdot w_e + 2{,}9895 \tag{6}$$

$$n = 2687 \text{ rpm} \qquad m_1 = -3{,}875 \cdot w_e^2 + 2{,}0592 \cdot w_e + 2{,}2914 \tag{7}$$

$$n = 1962 \text{ rpm} \qquad m_2 = 0{,}2401 \cdot w_e^2 - 0{,}8874 \cdot w_e + 1{,}2271 \tag{8}$$

$$n = 2325 \text{ rpm} \qquad m_2 = -2{,}3356 \cdot w_e^2 + 1{,}1042 \cdot w_e + 0{,}7711 \tag{9}$$

Relations from (6) to (9) describe the dependence of the parameters function shape of engine load.

Figure 9 shows the influence of engine speed and engine load on the relative duration of the first Vibe function. It may be concluded that engine load and engine speed do not have significant influence on the relative duration of the first Vibe function.

Figure 10 shows the influence of engine speed and engine load on the share of fuel mass burned as described by the first Vibe function. The values of this parameter are droping while engine load is rising.

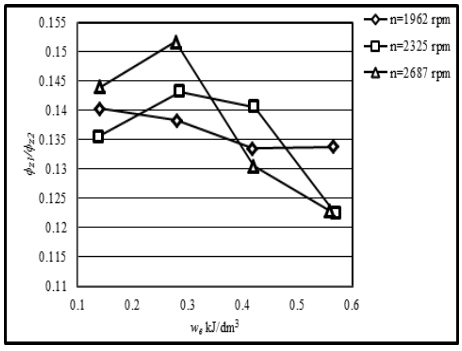

Figure 9 Influence of working regimes on duration of the first Vibe function

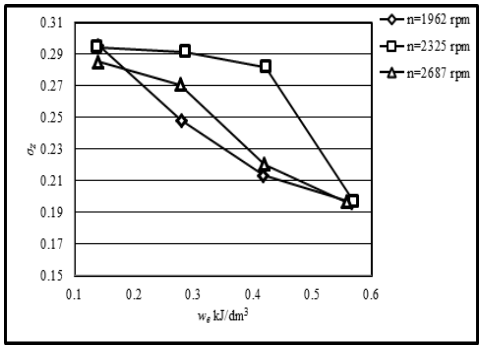

Figure 10 Influence of working regimes on the share of fuel mass burned during the first Vibe function

$n = 1962$ rpm $$\varphi_{z1}/\varphi_{z2} = 0{,}0302 \cdot w_e^2 - 0{,}0383 \cdot w_e + 0{,}1455 \quad (10)$$

$n = 2325$ rpm $$\varphi_{z1}/\varphi_{z2} = -0{,}3076 \cdot w_e^2 + 0{,}1885 \cdot w_e + 0{,}1151 \quad (11)$$

$n = 1962$ rpm $$\sigma_z = 0{,}4032 \cdot w_e^2 - 0{,}5194 \cdot w_e + 0.3608 \quad (12)$$

$n = 2325$ rpm $$\sigma_z = -0{,}9806 \cdot w_e^2 + 0{,}4821 \cdot w_e + 0.2434 \quad (13)$$

$n = 2687$ rpm $$\sigma_z = -0{,}1229 \cdot w_e^2 - 0{,}1407 \cdot w_e + 0.3102 \quad (14)$$

Relations from (10) to (14) describe the dependence of the duration of the first Vibe function and share of fuel mass burned during the first Vibe function of engine load.

CONCLUSIONS

In this paper is established that can define dependence between engine load and next parameters:

- shape parameter of first Vibe function m_2, and
- the share of fuel mass burned during the first Vibe function σ_z.

However some of the parameters cannot be defined by the equations, because of insufficient number of working regimes:

- shape parameter of first Vibe function m_1, and
- duration of the first Vibe function ϕ_{z1}/ϕ_{z2}.

The experiment is realized only on mono-cylindrical, air-cooled DI-diesel engine. Applicability of presented results on other diesel engines just is needed to check.

In the future can be going considered influence of other factors on double Vibe function parameters. For example: compression ratio, fuel characteristics…

Also in the case for diesel engines with modern injection systems, combustion process can be described with sum of more Vibe functions.

REFERENCES

[1] Radivoje B. PEŠIĆ, Aleksandar Lj. DAVINIĆ, Dragan S. TARANOVIĆ, Danijela M. MILORADOVIĆ, Snežana D. PETKOVIĆ, **Experimental determination of double vibe function parameters in diesel engines with biodiesel**, Thermal Science, ISSN 0354-9836, vol. 14 (2010), No. Suppl., pp. 207-218, DOI:10.2298/TSCI100505069P.

[2] J I Ghojel: Review of the development and applications of the Wiebe function: a tribute to the contribution of Ivan Wiebe to engine research, Department of Mechanical and Aerospace Engineering, Monash University, Wellington Road, Clayton Victoria 3800, Melbourne, Australia, (2010), DOI: 10.1243/14680874JER06510.

[3] A. Davinić, Ph. D dissertation: Indentifikacija karakteristika multiprocesnog rada klipnog motora SUS, Faculty of Engineering, University of Kрагујевац, 2013.

STRUCTURAL AND THERMAL ANALYSIS OF HEAVY VEHICLES' DISC BRAKES

Nadica Stojanović[1], *Jasna Glišović*

UDC:629.017:536.212

ABSTRACT: The effect of temperature and mechanical loads that occur when the vehicle is slowing down or stopping is shown in this paper. In the first section of paper, it is shown that with increasing temperature leads to decrease of the coefficient of friction i.e. the brake efficiency characteristics fade. The structural and thermal analysis is carried out on the model of brake disc and the brake pads, and the deformation and stress states of these elements are shown.

KEY WORDS: vehicle, coefficient of friction, deformation, stress.

STRUKTURNA I TERMIČKA ANALIZA DISK KOČNICA TERETNIH VOZILA

REZIME: Ovaj rad razmatra uticaj temperature i mehaničkih opterećenja koji se javljaju pri usporavanju ili zaustavljanju vozila. Na samom početku je prikazano kako sa porastom temperature opada koeficijent trenja, odnosno karakteristike kočenja blede. Na modelu je izvršena strukturna i termička analiza diska i kočnih pločica i prikazana su deformaciona i naponska stanja ovih elemenata.

KLJUČNE REČI: vozilo, koeficijent trenja, deformacija, napon.

[1] *Received October 2015, Revised November 2015, Published On Line December 2015*

Intentionally blank

STRUCTURAL AND THERMAL ANALYSIS OF HEAVY VEHICLES' DISC BRAKES

Nadica Stojanović[1], *Jasna Glišović*[2]

UDC:629.017:536.212

INTRODUCTION

Development of the brakes, as one of the key elements of vehicle's active safety, is based on the main requirement to keep a pre-set braking distance under various operation parameters. Experiences gained based on previous developed technologies have enabled the evolution of modern systems.

Disc brakes are a typical representative of the axial brakes, where the pressure on the friction surface is realized in the axis direction of the rotating element. As a disc rotates in free space, the assembly which is located in the calliper must be tightly closed and protected from contaminants from the environment and from water when driving in rainy weather. The caliper is in contact only with one part of the disc and not to the rest of the disc surface, which is of extreme importance because in this way provides efficient cooling [2].

The air braking system was originally designed for the railway vehicles [1]. They are today mounted on different types of heavy trucks, because of increased effectiveness in comparison to other brake systems. Here are just a few advanced features of air disc brakes:

- Brake solutions for all vehicle applications
- 20% to 30% better stopping performance and improved fade resistance over drum brakes
- Thicker pads mean enhanced durability and longer service intervals
- Proven durability and reliability for lower life cycle costs (longer pad and rotor life, less time to replace pads, environmental sealing integrity).

The friction pair - brake pad/disc has the basic task to produce the braking torque necessary to slow or stop the vehicle. However, in the braking process, the heat is generated. Brake pads absorb only a small amount of heat. This phenomenon is very useful in the braking process because it provides protection of the brakes and its internal components. The most of the heat generated during stopping is absorbed and temporarily stored by the disc but the disc capacity is limited. In order to maintain proper brake function, the disc also has the role of acting as a heat exchanger. Thereby, the disc may be able to dissipate the heat that is created in the process of braking into the environment. Solid disc has a limited, lower ability to remove heat. As a result, this simple design of disk has a smaller application on commercial vehicles. Ventilated discs with straight radial vanes and cross-drilled discs have been used in this type of vehicles. These elements allow air flows inside the disk and thus provide better heat dissipation.

[1] *Nadica Stojanović, PhD Student, Faculty of Engineering, University of Kragujevac, Sestre Janjić 6, Kragujevac, nadicasto@gmail.com*

[2] *Jasna Glišović, Assistant Professor, Faculty of Engineering, University of Kragujevac, Sestre Janjić 6, Kragujevac, jaca@kg.ac.rs*

THERMAL BOUNDARY CONDITIONS

Based on the first law of Thermodynamics, during braking, kinetic energy is converted to thermal energy. One of the main problems when designing brake is heat dissipation caused by friction that occurs in contact between brake pads and the brake disc. As can be seen from Figure 1, when the temperature of disc exceeds 700ºC, the coefficient of friction decreases rapidly, and it further leads to longer stopping distances [3]. At such high temperatures, pads suffer from a loss of effectiveness called "fade" because of a reduction in the kinetic friction coefficient. High interfacial temperatures can lead to a decrease in shear strength of the pad and consequently a decrease in frictional force which induces fade.

Due to friction between the main components of disc brake (pads and disc) the conversion of energy takes place. Initially, the generated thermal energy is transferred by conduction to the components in contact and next by convection and radiation to environment. In braking process, the temperature field changes input heat flux, and heat exchanges conditions. The input heat flux is mainly relevant to a disc coefficient of friction, the angular velocity of brake discs, while heat exchange is connected with the friction pair materials and external environmental factors.

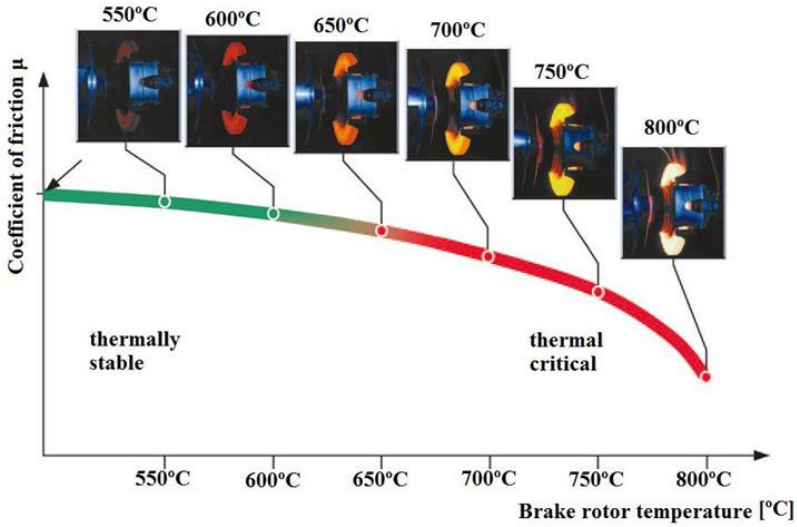

Figure 1 Influence of temperature on coefficient of friction [3]

STRUCTURAL AND THERMAL ANALYSIS

Stress condition of the disc at the effect of centrifugal force

Structural and thermal analysis was performed in the software package CATIA. Brake discs are exposed to a variety of loads during their use. While driving without braking the disc is affected only with the centrifugal force. When the brake process starts, two additional forces affect the disc. These forces represent the force from the brake calliper and the force from the heat impute (as a result of friction).

The material characteristics of the brake disc are shown in table 1.

Table 1 Material characteristics of venting disc [4]

	Ventilated disc
Young's modulus, E_d	195 GN/m^2
Poisson's ratio, υ	0,27
Density, ρ	7600 kg/m^3

In the beginning of the analysis, the brake disc is simplified. Only one section of the whole disc is used. Considering the systems edge conditions and the symmetry of the disc, only 1/4 of the disc is chosen.

The greatest stresses are in the zones where the disc is connected to the wheel with bolts, as well as on the inner surface of the disc, as shown in Figure 2.

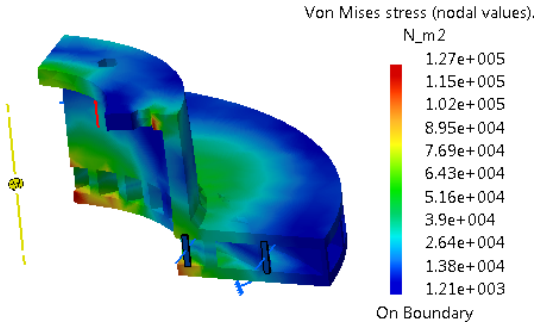

Figure 2 Stress on Von Mises that occurs as the effect of centrifugal force

Analysis of disc brake assembly

The ventilated disc is lighter than the solid disc, and additional convective heat transfer occurs on the surface of the vent hall. Thus, the ventilated disc can control its temperature rise and minimize the effects of thermal problems such as the variation of the pad friction coefficient, brake fade and vapour lock. The ventilated disc, however, may increase judder problems by inducing an uneven temperature field around the disc. Also, the thermal capacity of the ventilated disc is less than that of the solid disc, and the temperature of the ventilated disc can rise relatively faster than that of the solid disc during repetitive braking. Therefore, thermal capacity and thermal deformation should be carefully considered when modifying the shape of the ventilated disc.

Material properties friction pairs are given in Table 2, the angular speed of the disc is 200rpm.

Table 2 Material properties of friction pairs [5-7]

	Rotor	Friction material
Young's modulus, E_d	195 GN/m^2	3 GN/m^2
Poisson's ratio, υ	0,27	0,23
Density, ρ	7600 kg/m^3	2750 kg/m^3
Coefficient of friction, μ	0,4	0,4
Thermal expansion, δ	0,0000121 mm/K	-

Figure 3 Deformations of friction pair

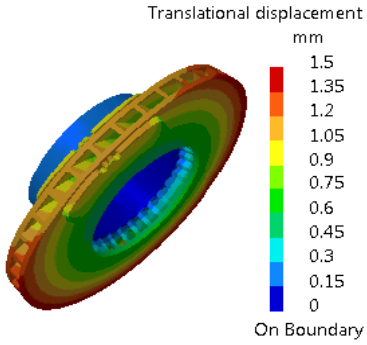

Figure 4 Translational displacement

Deformations of the disk are created as a result of thermal and mechanical loads. As shown in Figure 3, it can be noticed that disc under loads forms a specific shape that is known as the "umbrella effect". The effect of the umbrella is typical for integrally made discs. This phenomenon is a result from the heating of non-parallel paths of friction with respect to the initial position. Besides, the pads are also deformed. The internal pad is, contrary to the outside, less deformed. This occurs because the same pressure acts on the outer and the inner pads, and thereby the surfaces of the disc that are in contact with pads are deformed in direction of the wheel (to the outer side of the vehicle). As the disc deforms and begins to take the shape of the umbrella, the external pad has no room for an increase in cross-section direction, so this leads to the appearance of the compression. One can say that the deformation of the pad following the deformation of the disc.

The greatest translational displacements occur at the periphery of the disc, as a result of centrifugal force. In the case of brake pads, the largest translational displacement occurs in the upper part. Respectively, they follow the deformation of disc. More specifically, the inner pad is deformed outward, and this displacement is larger related to the deformation of the external pad, and as a consequence of disc deformation, the free space is remained, and pads take possession of it. The pressure acts on the outer pad on one side, and the disc being deformed acts from the opposite side. Due to the structural properties of the pad material, it follows the disk, and is deformed in the areas above the piston where it is pressed and thus enables it to fit on the disc. Translational displacement is higher for internal compare to external pad, Figure 4.

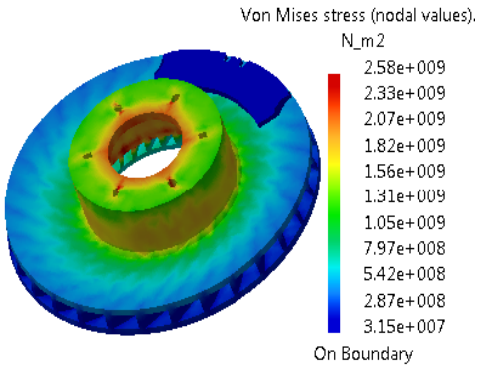

Figure 5 Von Mises stress of disc

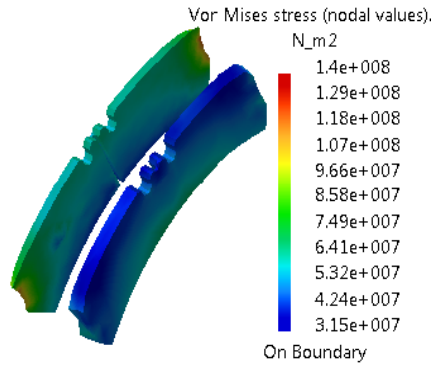

Figure 6 Von Mises stress of brake pad

The highest values of stresses occur in areas where the disc is in contact with the wheel and shaft, Figure 5. That is where the disc is screwed to the wheel flange and where it is in contact with the shaft. In these areas, the highest values of stresses occur because the wheels and shafts under the force of inertia tend to continue turning, until the disc along with the pads and the rest of the brake system does not allow. More precisely, it comes to the appearance of torsion.

Analysing the Figure 6 showing both the pads, apparently the highest stresses occur in the upper part of one pad, while in the other pad they occur in the bottom part. The reason is precisely the effect of an umbrella. This means that one pad with its upper end makes pressure and rest against with the disc, while the other pad rest with the bottom end and thus the braking force is transmitted from the pad to the disc.

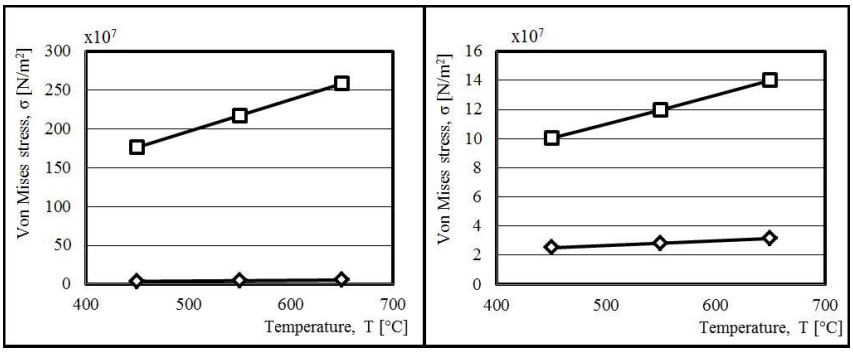

Figure 7 Min and Max Von Mises stresses that occur on the disc (left) and pads (right) in dependence of temperature change

By analysing the curves shown in Figure 7 it may be noted that the minimum values of Von Mises stresses for both the disc, and pads show a trend of the moderate increase with increasing temperature, and regarding the maximum value, that is not the case. So with an increase of the temperature, the maximum values of Von Mises stresses for disc and pads are rising rapidly.

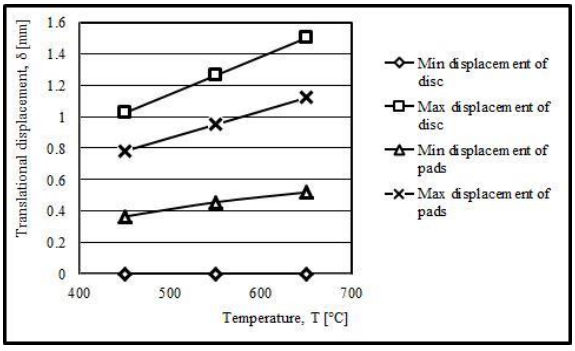

Figure 8 Min and max displacements that occur in the friction pair during temperature change

It can be concluded based on Figure 8 that the translational displacements increase with temperature. Minimum translational displacements of the disc are constant and they are equal to zero.

CONCLUSIONS

By analysing obtained results, it was found that disc due to the effects of high temperature and pressure (mechanical and thermal loads) that occur in contact between the pads and the disc, takes the form of the umbrella. It would be relevant for the further research to study in detail what would happen with integral ventilated discs. Furthermore, the air flow between disc's vanes is not taken into account in this paper i.e. the analysis was performed at room temperature, so it would be useful in future studies to take this aspect into account.

The data analysis has shown that the different stress values occur on the outside and inside pads, as well as translational displacements, and this can be considered. So it is possible to get stresses that occur on the inside and on the outside side of the pad. The same applies for translational displacement.

The analysis was carried out for the disc and pads, but for further research, it would be necessary to include other elements within the disc brake assembly, in order to determine the ways in which the heat is transferred to the other elements, by conduction, and convection. Of course, since the testing was performed on the disc and the brake pads made of most common materials for disc brakes of commercial vehicles, it can be analysed the influence of applying the new composite materials for disc and/or pads. In doing so, it would not be changed only the structural properties of the material, but also the coefficient of friction, thermal conductivity, etc.

REFERENCES

[1] European braking systems; Internet address: http://www.europeanbrakingsystems.co.uk/history, accessed 03.04.2015.
[2] Bendix Spicer Foundation Brake LLC; Internet address: http://www.foundationbrakes.com/media/documents/airdiscbrakes/awhitepapercaseforairdiscbrakes.pdf, accessed 03.04.2015.
[3] Breuer B., Karlheinz H. B.: Bremsenhandbuch-Grundlagen, Komponenten, Systeme, Fahrdynamik, Springer Fachmedien Wiesbaden, 2012, ISBN 978-3-8348-1796-9
[4] Ibrahim A., Analysis of disc brake squeal using a ten-degree-of-freedom model, International Journal of Engineering, Science and Technology Vol. 3, No. 8, 2011, pp. 142-155
[5] Parab V., Naik K., Dhale A. D., Structural and Thermal Analysis of Brake Disc, International Journal of Engineering Development and Research, Vol. 2, Issue 2, 2014, pp. 1398-1403
[6] Bayas E., Aher V., Coupled Field Analysis of disc Brake Rotor, International Journal of Advanced Research in Science, Engineering and Technology, Vol.02, Issue 01, 2012, pp. 06-09
[7] Lakkam S., Koetniyom S., Optimization of constrained layer damping for strain energy minimization of vibrating pads, Songklanakarin Journal of Science and Technology, Vol. 34, Issue 2, 2012, pp. 179-187

COMPARISON OF THE PHYSICAL AND EMPIRICAL APPROACH TO MODELLING OF QUASISTATIC ENVELOPING PROPERTIES OF THE TRACTOR TIRE

Boris Stojić[1]

UDC: 629.113;631.374; 631.565

ABSTRACT: Vibration properties of agricultural tractors are important indicator of their overall performances. Most important excitation source comes from pronounced short-wavelength road undulations, which are typical for unprepared off-road terrains generally dealt with by tractors. Low-pass geometric filtering of road profile done by tire thereby defines effective vibration input. Appropriate tire model that is able to account for this phenomenon is needed in order to optimize tractor vibration properties in early stage of development, by means of computer aided simulations with virtual prototype. To reduce tire model complexity and therefore improve simulation speed, yet achieving satisfactory accuracy, one possible approach is to separate tire model into two parts, one describing tire enveloping properties on the short-wavelength road input and the other one for tire elasticity with single-point contact. Enveloping model thereby generates effective excitation for contact point. In this paper two quasi-static tire enveloping models were derived. One of them is physically based and the other one is novel empirical model. Performances of both models are represented and compared with one another as well as with results of the physical experiment. Good agreement with experimental data is achieved in both cases. It was concluded that, in view of computational efficiency, empirical model manifested supremacy over physical model while the other one achieved greater flexibility regarding variations of influential parameters.

KEY WORDS: tractor vibrations, tire model, tire enveloping properties

POREĐENJE FIZIČKOG I EMPIRIJSKOG PRISTUPA MODELIRANJU KVAZISTATIČKIH ENVELOPNIH KARAKTERISTIKA PNEUMATIKA TRAKTORA

REZIME: Vibracione karakteristike poljoprivrednih traktora su važan pokazatelj njihovih ukupnih performansi. Najvažniji izvor su neravnine puta male talasne dužine, koje su tipične za nekategorisane puteve i vanputne podloge karakteristične za traktore. Pneumatik vrši nisko propusno filtriranje profila puta i to je značajna vibraciona pobuda. Odgovarajući model pneumatika koji je u stanju da objasni ovaj fenomen je potreban u cilju optimizacije vibracionih karakteristika traktora u ranoj fazi razvoja, pomoću računskih simulacija na virtuelnim prototipu. Radi smanjenja složenosti modela pneumatika i poboljšanja brzine simulacije, i postizanja zadovoljavajuće tačnosti, jedan od mogućih pristupa je da se model pneumatika razdvoji na dva dela: jedan koji opisuje karakteristike envelope pneumatika izloženog neravninama kratkih talasnih dužina i drugi koji opisuje elastičnost pneumatika sa kontaktom i tački. Model envelope generiše efektivnu pobudu u tački. U ovom radu su prikazana dva razvijena kvazistatička modela pneumatika. Jedan od njih je fizički, a drugi

[1] *Received September 2014, Accepted October 2015, Published On Line December 2015*

je empirijski model. Performanse oba modela su predstavljene i upoređene jedne sa drugima kao i sa rezultatima fizičkog eksperimenta. Dobro slaganje sa eksperimentalnim podacima je ostvareno u oba slučaja. Zaključeno je da, s obzirom na računsku efikasnost, empirijski modeli manifestuje bolje karakteristike fizičkog modela, dok drugi daje bolje mogućnosti za variranje uticajnih parametara.

KLJUČNE REČI: vibracije traktora, model pneumatika, karakteristike envelope pneumatika

COMPARISON OF THE PHYSICAL AND EMPIRICAL APPROACH TO MODELLING OF QUASISTATIC ENVELOPING PROPERTIES OF THE TRACTOR TIRE

Boris Stojić, Ph. D, Assistant professor

UDC: 629.113;631.374; 631.565

INTRODUCTION

Tractor tire vibration characteristics are an important indicator of their overall performance. Tractors mostly travel off-road with the presence of shock barriers and short-wavelength unevenness what emphasise the ability of tires to deform locally and envelope the obstacle – 'enveloping behaviour'. As a result, vibration excitation transmitted to the tractor does not match the actual surface profile but occurs as a result of geometric filtering of the actual profile. In spatial domain, this excitation is represented by the trajectory of tire's centre point and it is called the effective profile of the surface or enveloping curve. Therefore, the enveloping curve is defined by dependence between the ordinate height of the effective profile and longitudinal position of the tire. In the study of vibration behavior of the tractor using the computer aided simulation it is necessary to have available the tire model that is able to cover the above phenomenon. Possible approach is to use an analytical model of the tire structure which, taking into account geometrical and physical properties of the actual tire, can predict local deformities of the short-wavelength unevenness and therefore, the effective micro profile. Having in mind that such models are based on the real structure of the tire they are usually characterized by a high degree of complexity. This complexity can have a negative impact on the speed of simulation what can be seen as a disadvantage. This problem can be eliminated by using an alternative approach. This paper discusses the concept of dividing an integral tire model into two basic components:

- model of elastic structure
- enveloping model.

This approach allows the development of a simpler model, and hence shorter execution time. In order to circumvent the difficulties in analytical modeling of the contact that tires have with uneven terrain a semi-empirical or empirical approach can be used for an enveloping model [9][13].

The aim of this paper is development and application of two different enveloping models and their comparative analysis. One model is empirical in nature, based on artificial neural network and the other analytical, based on a simplified tire structure (radial and interradial springs).

TIRE ENVELOPING BEHAVIOR

Rolling over short-wavelength unevenness ie. those with length less than the tire contact length, the tire performs low-pass geometric filtering of the ground profile. According to [13], the effect of filtering is based on the following mechanisms:

1.When the tire rolls over the short wave-length unevenness its front segment will, based on geometric conditions, come into contact with an uneven terrain before the central area of the

tire comes over that edge. Because of the tire symmetry the same conclusion (but in reverse) applies to the completion of the tire contact and an uneven terrain after the posterior segment of the tire crosses over. Accordingly, the length of a particular segment of the effective profile is greater than the length of its corresponding unevenness.

2.When the tire crosses over a discreet unevenness, whose length is less than the tire contact length due to the effects of vertical force and thanks to tire structure compliance, the contact surface is locally deformed partially or completely enveloping the uneven terrain. As a result, the maximum height reached by the tire center when overcoming unevenness remains less than the height of the unevenness.

3.The third mechanism, based on both geometry and the effect of local deformities, is the transformation of sharp, singular edges of the observed unevenness into smooth segments of the enveloping curve.

There have been numerous research of pneumatic tire behaviour on uneven terrain carried out by a number of authors, for example [1][4][8][9][13] etc. Typical form of response to an obstacle of a rectangular cross-section with a vertical wheel load as a parameter is shown in Figure 1.

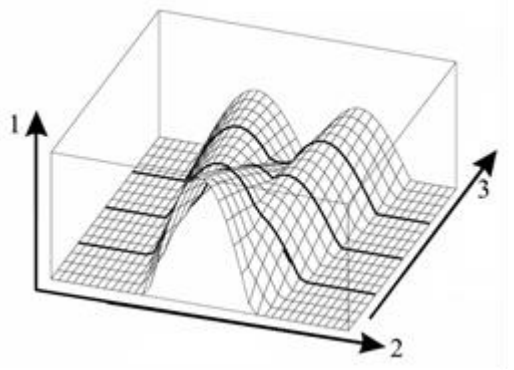

Figure 1 Typical response of pneumatic tire on rectangular obstacle with vertical wheel load as parameter [13]:

1 – effective road profile height, 2 – longitudinal displacement, 3 – vertical wheel load direction

EXPERIMENTAL FACILITY

Experimental research necessary to gather empirical data was carried out by experimental facility whose simplified scheme is shown in Figure 2. The facility is based on a rail guided cart which rolls a vertically movable frame with a tire to be tested. That way the tire can also move in the vertical direction while rolling over uneven terrain and generating effective profile. Thus, in the case of quasistatic conditions, the vertical ground reaction remains constant during the motion. Record of effective surface profile is obtained by simultaneous measurement of longitudinal and vertical coordinates of the tire center. Such experimental facility was described in more detail in previous publications, eg. [10], [11].

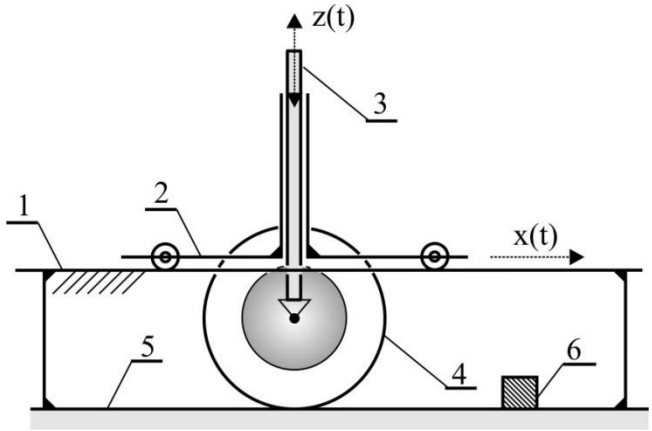

Figure 2 Simplified schematics of experimental facility: 1-rails, 2-cart guiding the tire, 3-vertical tire guide, 4-testing tire, 5-flat surface, 6-obstacle (uneven terrain); x(t), z(t)-longitudinal and vertical movement of tire, respectively

A rectangular cross-section obstacle was used in experimental research and the results obtained using these obstacles are proportionally easy to interpret and compare. Rectangular cross-section obstacles are greatly used in the studies of other authors (eg. [8], [9], [13], etc.) since they are well suited for standardization and their relatively easy application in the real and virtual tests.

NEURAL NETWORK-BASED TIRE ENVELOPING MODEL

Effective profile is based on local deformations of tires in contact with the short-wavelength unevenness. This occurrence s accompanied by a variety of mechanisms and phenomena of a complex nature. There are the following phenomena: nonlinearity of geometry, nonlinearity of material behavior, anisotropy of composite structure, viscoelasticity of rubber compound etc. Because of all this, the analytical modeling of the observed phenomena leads to various problems. An alternative approach is the adoption of empirical modeling approach, thus forming a suitable mathematical relationship that connects the input to the output data, without taking into account the physical nature of the observed system or phenomenon. Neural networks are structures of artificial intelligence capable that through training and iterative application of an appropriate optimization algorithm, establish the required input-output relation. Among other things, their use is especially expedient in the case of empirical modeling of phenomena which exhibit a high degree of complexity and nonlinearity [3].

To form a model a feed-forward, back propagation neural network was chosen as a form of neural network suitable for establishing an empirical input-output relation. Since the enveloping curve defines dependence between the tire longitudinal position as input and height ordinate of effective profile as the output values, thus partially defining input and completely defining output from a neural network. Input data must be completed by the tire longitudinal coordinate and the obstacle geometry parameters, if the neural network is to be trained for obstacles of various dimensions.

In order to find optimal parameters for a neural network and its training process there are no unambiguously defined criteria. Therefore, it is necessary to apply an experimental approach which means parameters have to be varied until reaching an optimal solution. In order to achieve that it is necessary to define:

•optimal network structure ie number of hidden layers and number of neurons in them
•optimal training data set
•optimal number of learning cycles

Due to all of the above the training process can be lengthy and complex. On the other hand, in the stage of application, a model based on neural network is characterized by a relatively high speed of execution. Adopted structure and characteristics of the neural network, with structure schematic in Figure 3, is shown in Table 1. Basic characteristics of the training process are given in Table 2. In addition, each of the data sets listed in Table 2 consist of a set of discrete, associated values of input and output vectors at quasistatic tire roll over obstacles, starting with the establishment of the initial contact to the position in which the vertical axis of symmetry of the tire and an obstacle are congruent. Such choice of length was made on the basis of symmetry of enveloping curve compared to vertical axis.

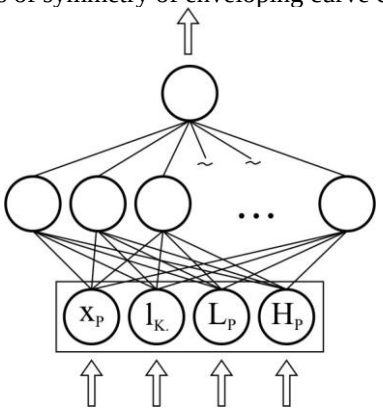

Figure 3 Feed-forward neural network schematic

Table 1 Basic characteristics of neural network

Type of network	Feed-forward, backpropagation
Number of input neurons	4 (normal longitudinal movement, tire working regime parameter, obstacle height, obstacle length)
Number of hidden layers	1
Number of neurons in a hidden layer	8
Number of output neurons	1 (effective road profile height)
Connectivity	Complete forward directed connectivity of adjacent layers
Training algorithm	Standard Backpropagation algorithm
Activating function	Logistic function, $f(x) = 1/(1+e^{-x})$
Exit function	Identity, $f(x) = x$

Table 2 Basic characteristics of training process

Number of available training sets (number of different obstacles)	28
Number of data sets used for training	19 (≈68%)
Number of data sets used for control of generalisation ability during training	5 (≈18%)
Number of data sets used for validation	4 (≈14%)
Number of training cycles	$\approx 2 \cdot 10^5$

TIRE ENVELOPING MODEL WITH RADIAL AND INTERRADIAL SPRINGS

Tire model with a system of radial springs, to which interradial ones can be added, is an analytical (physical) model based on the simplification and discretization of tire elastic structure. In this model radial springs present radial structure elasticity while interradial springs mould bending stiffness of a tire tread. This concept has been previously known and used in literature, for example [1], [12] and others. In this paper, model application was adapted to the quasistatic conditions ie. tire rolling is modeled over an obstacle at a constant intensity of a vertical ground force.

The model is based on a curved segment with a number of radial and interradial springs, according to Figure 4 (a).

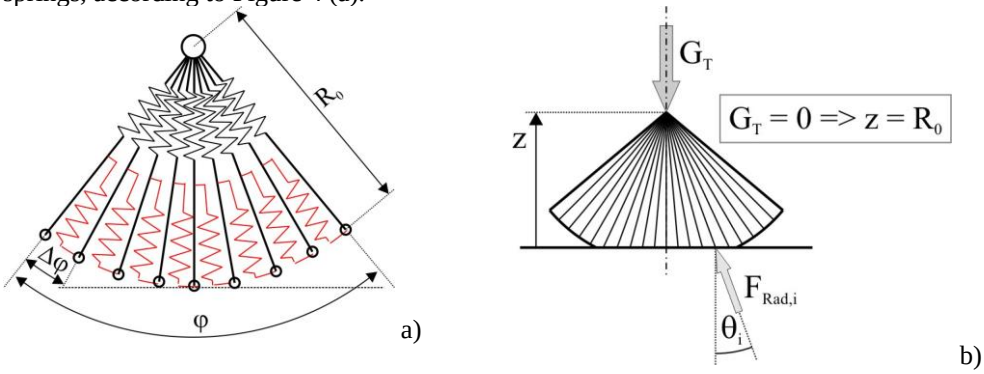

Figure 4 a) Geometric form of a model with radial and interradial springs: R_0 – free tire radius, φ - angular segment width, $\Delta\varphi$ - angle between adjacent radial elements

b) The effect of vertical load GT on a model: FRad,i – force in the i^{th} radial element; θ_i – angle between the vertical axis and force line of application FRad,i; z – coordinate defining the position of the system relative to vertical axis

Vertical load pressures tire tread segment causing deflection of some radial elements and the formation of radial forces. Static equilibrium in the vertical direction is of importance in this case and its equation is:

$$G_T = \sum F_{Rad,i} \cdot \cos\theta_i \,, \tag{1}$$

Sum in (1) applies to all elements whose deflection is greater than zero or who were deformed under the influence of load GT. When communicating or changing the vertical load, the position of the system changes due to the response of radial and interradial elements. As elements are subjected to deflection ie with the increase in vertical load, they successively come into contact with the surface, it is not possible to analytically solve a system of constitutive equations since there is no advance knowledge of the number of elements, realizing static equilibrium, that will tread the surface. Therefore, it is necessary to use an iterative approach in order to find an approximate balance position.

For each longitudinal position through which the system passes during the simulation iterative calculation of static equilibrium position is carried out. Iterative procedure starts from the coordinate z guess value and the current value of the longitudinal position x. For these values of x and z deflection of radial elements is calculated and memorized from geometrical conditions providing radial force values. By summing up the vertical components of certain forces a total surface reaction for a given system position is calculated. If there is a deviation between the calculated and the given value of the surface response (which, due to static equilibrium must be equal to GT) that is greater than a preset permitted tolerance □, then a new value of coordinate z is calculated in accordance with secant method for iterative solution of the nonlinear equations [6]:

$$\left|G_T - F_{Z,sum}\right| > \varepsilon \Rightarrow z_{(j+1)} = z_{(j)} - \frac{\left(F_{Z,sum(j)} - G_T\right)\left(z(j) - z(j-1)\right)}{F_{Z,sum(j)} - F_{Z,sum_{j-1}}}, \qquad (2)$$

where:

- j – serial number of iteration steps

Model parameters are stiffness coefficients of radial and interradial springs, as well as the number of radial elements. The optimal parameter values are determined by experiments, by variations in certain number of iterations.

MODELS COMPARISSON

Performance analysis of the models and their comparison was made on the basis of model prediction review together with the review of certain measurement results, Figure 5. The covered cases (in terms of various obstacle dimensions and tire working regime) are shown in Table 3.

Table 3 Results used for comparison and performance analysis of the models

Serial number	Label (internal)	Tire working regime indicator – contact length (mm)	Obstacle dimensions(length × height, mm)
1	"F"	380	300 × 100
2	"J"	330	300 × 50
3	"R"	280	100 × 100

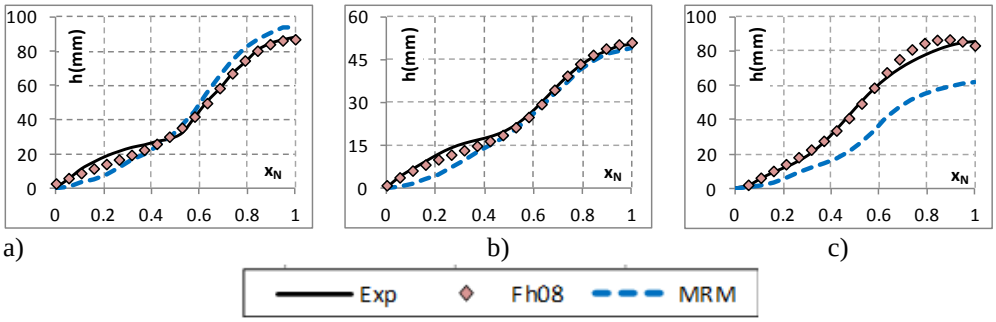

Figure 5 Simulation results comparison of empirical and physical model with measuring results according to Table 3 a) case 1, b) case 2, c) case 3h(mm) – effective surface profile height, xN – normalized longitudinal displacement

Figure 5 shows that the empirical model qualitatively provides a satisfactory description of the real system behaviour, while the physical model exhibits some discrepancies in the initial part of the curve (near the origin). These deviations, however, occur in the area of small amplitudes and therefore, can be expected not to impair the overall prediction accuracy of the model significantly.

Regarding the quantitative accuracy of the predictions, Figure 5 a) and b) (cases 1 and 2 of Table 3, respectively) show that in these cases, with the approximate degree of accuracy, both models describe the enveloping curve but the empirical model achieves slightly better results. In case c) in Figure 5 (case 3 in Table 3) for both models the results are worse than in the previous cases and the physical model prediction totally deviates from the measurement results. The results suggest that the assumption regarding the physical model degree of discretization should be adapted to the geometry of the surface profile. Also, it can be concluded that both models have difficulties with modeling tire response to obstacles with height and length ratio above a certain threshold..

CONCLUSIONS

In this paper two models of quasistatic enveloping curve of tractor tires were developed. The empirical model, based on artificial neural network, is an original solution to the problem in a way that it has not been applied in previous research. The physical model is based on discretization and simplification of the tire physical structure by representing it as a system of springs. This model, used by other authors (eg. [1], [12] and others.), was suited for quasistatic enveloping curve modeling in this study.

The empirical model is characterized by high-speed execution in the application stage and that is its most important asset. Since this is a model based on artificial neural networks in the stage of model generating it was not necessary to perform parameterization procedure. The main disadvantages of the model are the need for intensive work on experimental measurements and time-consuming, experimentally based, parameter optimization process of neural network as well as its training. Also, the model does not have the flexibility to adapt to change the structural parameters of the tire. The model is suitable for application within the simulation of vertical dynamics of the tractor when traveling over uneven terrain.

Carrying out a physical model involves an iterative process causing its significantly lower speed of performance. One of the model's advantages is the possibility to change the numerical values of parameters for tire modeling of different structural characteristics. Also, model parameterization requires a relatively small number of experimental measurements.

On the other hand, parameterization is based on an experimental approach and that makes the whole process lengthy and complex. The structure of the model developed in this study cannot be directly applied in a vehicle dynamics environment since it is a quasistatic model. The purpose of this model is to use its results in the empirical model training and thus save labour and time for experimental testing.

As far as the accuracy issue is concerned, to some extent exhibited by both models, especially the physical one, it should be noted that this study carried out a preliminary model development. It can be expected that the accuracy will be improved by further development of both models. Further study will include, in addition to model training, the application of the empirical model within the vehicle dynamics simulation and its integration with the model of the elastic tire structure.

ACKNOWLEDGMENTS

This research was done as a part of project TR35041 "Investigation of the safety of the vehicle as part of cybernetic system: Driver-Vehicle-Environment", supported by Serbian Ministry of Science and Technological Development.

REFERENCES

[1] Badalamenti J. M., Doyle G. R.: Radial-Interradial Spring Tire Models, Journal of Vibration, Acoustics, Stress and Reliability in Design, 110(1988)1, 70-75

[2] Herkt S.: "Towards a Finite Element Tyre Model for Multibody Simulation", Dissertation, Universität Kaiserslautern, 2008, Kaiserslautern, D

[3] Kinnebrock, W.: Neuronale Netze – Grundlagen, Anwendungen, Beispile, R. Oldenbourg Verlag München Wien, 1992.

[4] Maurice, J.P.: "Short Wavelength and Dynamic Tyre Behaviour under Lateral and Combined Slip Conditions", PhD Thesis, Technical University of Delft, Netherlands, 2000, Delft, NL,

[5] Oueslati F.: "An Analytical Investigation of Passive and Active Suspension Systems for Articulated Freight Vehicles", PhD thesis, Concordia University Montreal, Quebec, 1995.

[6] Petković Lj.: Numerička matematika sa programiranjem, Gradina, Niš, 1994.

[7] Scarlett, A.J. et al: "Whole-body vibration on agricultural vehicles", Research report, Silsoe Research Institute and RMS Vibration Test Laboratory for the Health and Safety Executive, 2005, Silsoe, GB,

[8] Schlotter V.: Einfluss dynamischer Radlastschwankungen und Schräglaufwinkeländerungen auf die horizontale Kraftübertragung von Ackerschlepperreifen, Dissertation, Universität Stuttgart, 2005.

[9] Schmeitz, A.J.C.: "A Semi-Empirical Three-Dimensional Model of the Pneumatic Tyre Rolling over Arbitrarily Uneven Road Surfaces", PhD Thesis, Technical University of Delft, Netherlands, 2004, Delft, NL,

[10] Stojić B., Poznić A., Časnji F.: "Test Facility for Investigations of Tractor Tire Dynamic Behavior on Hard Surfaces", 39th International Symposium: "Actual Tasks on Agricultural Engineering", 2011, Opatija, HR, 119-127

[11] Stojić B., Poznanović N., Poznić A.: "Test Facility for Investigations of Quasistatic Enveloping Behavior of Tractor Tire", 8th International Symposium "Machine and Industrial Design in Mechanical Engineering", 2014, Balatonfüred, HU, 89-92

[12] Witzel,P., Böttinger,S.: Upgrading of the Hohenheim Tyre Model to a radial approach for the simulation of obstacle passages, VDI Berichte Nr. 2124, VDI-Verlag, Düsseldorf, 2011, 431-437

[13] Zegelaar, P.W.A.: "The Dynamic Response of Tyres to Brake Torque Variations and Road Unevennesses", PhD Thesis, Technical University of Delft, Netherlands, 1998, Delft, NL.At annual and total level in production processes of the new fabrics for vehicle production.

TRIBOLOGICAL OPTIMIZATION OF RECIPROCATING MACHINES ACCORDING TO IMPROVING PERFORMANCE

Saša Milojević[1], *Radivoje Pešić, Dragan Taranović, Aleksandar Davinić*

UDC:629.014.6

ABSTRACT: Lowering fuel consumption and exhaust emissions continue to be prime targets in the development of technology applied for Motor Vehicles and their equipment. Into the focus of attention are the reduction of the vehicle weight as well as, in the field of internal combustion engine technology, more efficient combustion system and accessory components.

As a complex system, the internal combustion engine accounts for a major part of the vehicle mass. The key components, the cylinder head and the cylinder block, for heavy loaded diesel engines, are today almost exclusively produced from aluminium. Also, by application of the aluminium pistons, it reduces engines' weight and inertial forces, as well as the engine vibrations. According to the later, the use of lightweight materials for construction of engine's accessories as it is small air reciprocating compressor for braking system of trucks and buses, has significant contributions to the reduction of equipped vehicle mass.

The advantage of aluminium with regard to the specific weight is notable, but exist the problem because it has considerable disadvantages in terms of the thermal expansion coefficient. The greater thermal expansion would cause unacceptable deformation and higher clearances during reciprocating machine operations. These high clearances would drastically increase the oil consumption and worsen the acoustic excitation. With additional coating on the cylinder liner surfaces it overcoming of poor aluminium strain properties. The application of tribological inserts towards lowering friction resulting in higher performance. The authors hope to obtain more measurement data on the test rig for small air reciprocating compressors in the Engine Laboratory at the Faculty of Engineering University of Kragujevac, which is currently being brought into operation.

KEY WORDS: Reciprocating aluminium machines, Plasma spray coating, Lowering friction

POBOLJŠANJE PERFORMANSI KLIPNIH KOMPRESORA TRIBOLOŠKOM OPTIMIZACIJOM

REZIME: Smanjenje potrošnje goriva i emisije izduvnih gasova i dalje će biti glavni ciljevi u razvoju tehnologija koje se primenjuju kod motornih vozila i njihove opreme. U centru pažnje je smanjenje težine vozila, kao i u polju razvoja tehnologija motora sa unutrašnjim sagorevanjem, primenom efikasnijeg sistem za sagorevanje i pomoćnih komponenata

Iako je složen sistem motor sa unutrašnjim sagorevanjem motor predstavlja značajan deo ukupne mase vozila. Najvažnija komponenta, glava cilindra i blok cilindra, kod teško opterećenih dizel motora, danas se isključivo proizvode od aluminijuma. Dakle, primenom aluminijumskih klipova, smanjuje se težina i vibracije motora. Primena lakih materijala za

[1] *Received: September 2014, Accepted October 2014, Available on line December 2015*

izgradnju motora i opreme kao što je mali klipni kompresor kočionog sistema kamiona i autobusa, ima značajan doprinos smanjenju ukupne mase vozila.

Prednost aluminijuma u odnosu na specifičnu težinu je evidentan, ali ima nedostatke u pogledu značajnog koeficijenta termičkog širenja. Što je veće termičko širenje dolazi do većih deformacija ali i većih zazora u procesu rada klipnih kompresora. Ovi visoki zazori dovode do značajnog povećanja potrošnje goriva i povećanja akustičkih pobuda. Sa dodatnim premazom površine cilindarske košuljice poboljšavaju se deformacione osobina aluminijuma. Primena triboloških umetaka za smanjenje trenja dovodi do boljih performansi. Autori se nadaju da će dobiti više podataka iz ispitivanja na mernom mostu za ispitivanje klipnih kompresora koji je razvijen u Laboratoriji za motore Fakulteta inženjerskih nauka Univerziteta u Kragujevcu, koji se trenutno uvodi u rad.

KLJUČNE REČI: Klipni aluminijumski kompresor, Plazma prevlake, smanjenje trenja

TRIBOLOGICAL OPTIMIZATION OF RECIPROCATING MACHINES ACCORDING TO IMPROVING PERFORMANCE

Saša Milojević[1], Radivoje Pešić[2], Dragan Taranovic[3], Aleksandar Davinić[4]

UDC:629.014.6

INTRODUCTION

Society relies on reciprocating machines for transportation, commerce and power generation: Internal Combustion Engines (ICEs), utility devices (e.g., compressors, pumps, portable generators, etc.). ICEs power the world's fleet of vehicles, which is passed number of one billion passenger cars and other vehicles on our roads today.

In gasoline-powered vehicles, over 62% of the fuel's energy is lost in the ICEs. IC engines are very inefficient at converting the fuel's chemical energy to mechanical work, losing energy to engine friction, pumping air into and out of the engine, and wasted heat. Advanced engine technologies such as variable valve timing, turbocharging, direct fuel injection, and cylinder deactivation can be used to reduce these losses. In addition, diesels are about 30-35% more efficient than gasoline engines [10,11].

The popularity of Diesel engines in passenger cars is the result of their economy and improved drive ability in recent years. Diesel engines necessitate high peak cylinder pressure to ensure an appropriate torque and performance, together with low consumption and improved exhaust gas emissions. Al the more since an additional reduction of engine weight is required. Lightweight design has two goals: Fuel economy due to a lighter vehicle on the one hand and weight distribution in the vehicle (driving dynamics) on the other hand. Generally, Diesel motorization constitutes the heaviest assembly (robust construction, turbo charger, charge air cooler, fuel-injection equipment), so that the balance gets affected by the excess weight on the front axle.

At the core of these conflicting goals is the heaviest single component of the engine, the engine block and engine's accessories (water pump, alternator, fans, air reciprocating compressor …).

As example, a long list of clean technologies was reviewed for application for buses, grouped into vehicle, powertrain and fuel themes, Table 1.

Inside of powertrain system, engine efficiency is a main area for clean technologies grouped into four themes [11]:

- Combustion Systems (Injection optimization, Exhaust Gases Recirculation (EGR), Optimized Inlet Swirl, Early End of Combustion, Low Exhaust Back Pressure, Boosting, Inlet Manifold Temperature Control,

[1] *mr Saša Milojević, Assistant R&D, Faculty of Engineering University of Kragujevac, tiv@kg.ac.rs*
[2] *dr Radivoje Pešić, full prof. University of Kragujevac, Faculty of Engineering, pesicr@kg.ac.rs*
[3] *dr Dragan Taranović, prof. assist. University of Kragujevac, Faculty of Engineering, tara@kg.ac.rs*
[4] *dr Aleksandar Davinić, prof. assist. University of Kragujevac, Faculty of Engineering, davinic@kg.ac.rs*

- Friction reduction (Lubricant Viscosity Specification, Piston ring design, Plasma coated cylinder liner, Piston skirt – design and coating, Crank/cylinder axis offset, Bearing design),
- Engine Accessories (Reduction in parasitic losses of engine accessories; Air reciprocating compressor – flow optimization and electric clutch, variable flow and electric oil pump, electric water pump), and
- Gas Exchange (Electric assisted turbocharger, Variable valve actuator, EGR pump).

Table 1 *Example of low carbon technologies applicable for city buses [11]*

Technologies	Control Measures
Vehicle	• Reducing vehicle drag: Low rolling resistance tires, aerodynamic body modification • Light weighting • Predictive cruise control, platooning and driver behavior
Powertrain	• Engine: Combustion system and gas exchange system improvements, engine downsizing, lubricants for engine friction reduction, fuel additives • Parasitic losses reduction: variable flow oil and water pump, clutched compressor, smart alternator, variable speed fans • Waste heat recovery/ thermal management: Mechanical and electrical turbo compound, thermoelectric generators… • Driveline: Automated manual transmission, Continual Variable Transmission CVT • Hybridization: start stop, mild hybrid, series and parallel electric and hydraulic hybrids
Fuel	• Alternative fuels: Hydrogen (IC engines and fuel cell), electricity • Cleaner fossil fuels: Compressed natural gas … • Biofuels: Compressed biogas

Inside of the paper is presented the analysis regarding to the optimization of air reciprocating compressors as a contribution to reduction in parasitic losses of IC engine's accessories. Test-bench has been carried out inside of Laboratory for IC engines at University of Kragujevac, Faculty of Engineering, on a single cylinder aluminum compressor. An example how to reduce the friction by application of tribological inserts will be outlined. More details on the compressor performance and design changes made to the cast aluminum cylinder and piston, as well as cylinder head in order to take full advantage of the coating is presented in the paper from Pešić et al. [7].

STATE OF THE MATERIAL TECHNOLOGY IN PRODUCTION OF LIGHTWEIGHT METAL CYLINDER HEADS AND ENGINE BLOCKS

Modern high-performance engines place highest demands on the mechanical and physical properties of the cylinder head and the engine block. The high combustion pressure in the diesel engines require a material with extremely high tensile strength and creeping strength, thermal conductivity, ductility and elasticity combined with high thermal shock resistance and cast ability combined with low susceptibility to hot cracking.

Honing structures are being optimized on existing, proven cylinder surfaces such as cast iron blocks and sleeves, hypereutectic aluminium alloys (Alusil®), and on various galvanic coatings (e.g. Nikasil®). In parallel, the direct coating of cylinder liner surfaces

with the application of thermal spray processes has become more and more important. Applying a coating directly to the cylinder surfaces in aluminium engine blocks can eliminate the need for cast iron sleeves. This can significantly reduce the weight of the engine block; leads to improved heat transfer from the combustion chamber into the cooling medium and can give corrosion protection of the liner surface.

Cylinder Heads

The complexity of the cylinder heads, specifically for the heavily loaded diesel engines with direct fuel injection, as well as the stress load during operation has increased significantly. The central part of the cylinder head near the combustion chamber and exhaust valve(s) are additionally subject to high temperatures ranging between 180 and 220 0C and above. In these temperature ranges can exist the mechanical problems due to fatigue strength, resulting the formation of cracks in these critical zones [2].

As an example, during the development of the alloys for the cylinder heads of the Audi V6 and V8 diesel engines, following alternative alloys examined [2]:

- ALSi12CuNiMg (primary alloy; the component features very good resistance to cracking, but during casting it is very susceptible to hot cracking)
- ALSi7MgCu0.5 (primary alloy; good predictability of the mechanical properties and good resistance to cracking combined with very good cast ability)
- ALSi9Cu3 (secondary alloy; very good mechanical properties combined with good cast ability).

Cylinder heads of these three alloys were examined with a view to their mechanical properties after a residence time of 230 to 240 h at 225 0C. All alloys exhibit a distinct decline in strength accompanied by increasing elongation after fracture, Figure 1 [2].

Engine tests with ALSi7MgCu0.5 provided good results for all simulated load situations [2]. Although the price for this primary alloy is slightly higher, for this application it can be considered as an ideal compromise between strength, behaviour at elevated temperatures and thermal conductivity. It guarantees, with a sufficient degree of reliability, the functioning of the cylinder head throughout its designed lifetime.

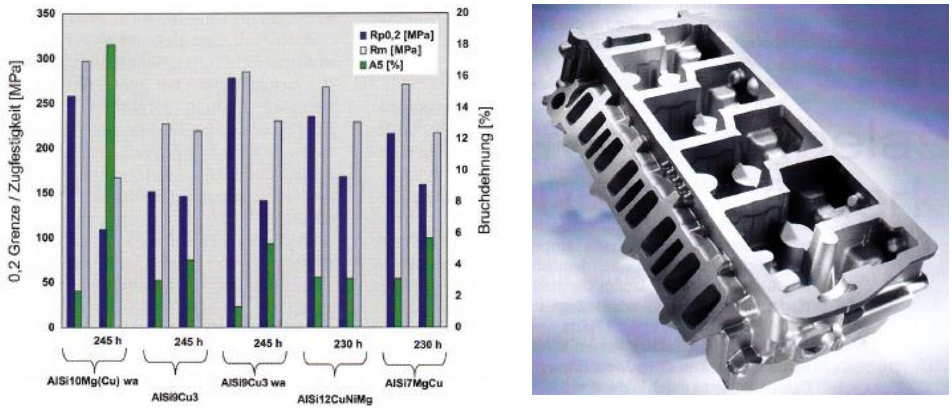

Figure 1 (a) Mechanical properties, of different casting alloys after approx. 240 h at 225 0C

(b) Cylinder head for the Audi 4.0-L V8 TDI engine in the ALSi7MgCu0.5 alloy, weight approx. 13 kg [2]

ENGINE BLOCKS

The weight of the cylinder block accounts for approx... 25 to 33% of the total engine weights depending on the size and design of the engine, the type of combustion process and the design of the crankcase. Especially, for the mass production of aluminium engine blocks most diverse concepts are used.

The strains acting on the engine block are illustrated in Figure 2. The increased specific power output leads primarily to a higher thermal strain of the cylinder liner. The direct heat induction by the combustion gas and the indirect heat induction by piston and rings particularly affect the upper part of the cylinder. As far as aluminium is concerned, its deformation due to temperature strain and the deterioration of its material properties at increased temperature (inter-bore section) have to be taken into account. In the crankcase area, where the bearing forces of the crankshaft occur, the strain rises in direct proportion to the peak pressure. Moreover, a dynamic layout of the crankcase is necessary because of the crankshaft deflection and the transmission of the combustion noise through the crank train (inner noise transfer path). The engine block must not only stand the thermo mechanical strain, but it is also supposed to form a tribological suitable bearing surface for the piston [8].

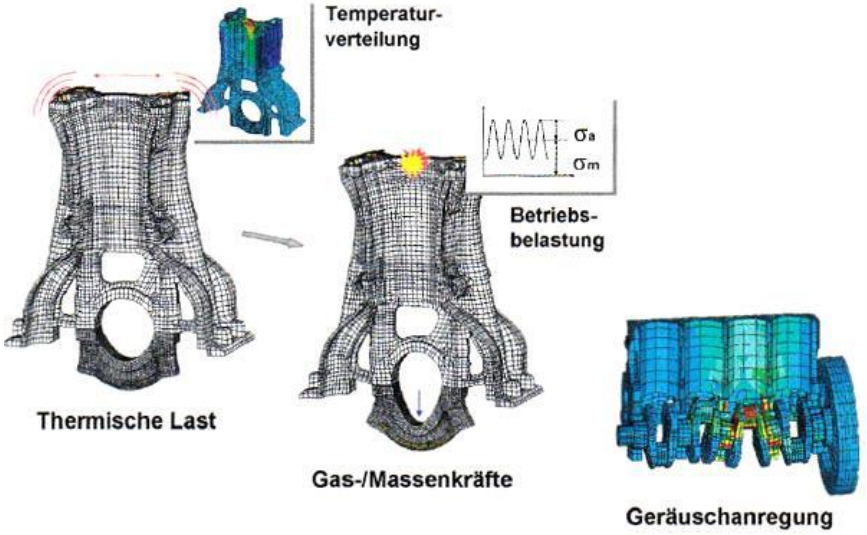

Figure 2 *Loading of the engine block*

As example, one material that combines almost all necessary properties is lamellar grey cast iron (GJL) or (Der lamellare Grauguss). GJL usually possesses sufficient strength and offers good tribology qualities for the cylinder liner. Its casting and processing properties are advantageous, too Figure 3. The major disadvantage of GJL material is its specific weight. The vermicular graphite cast (GJV) or (Der Vermikulargraphitguss), shares this disadvantage, but it possesses conspicuously higher degrees of stiffness and strength [8].

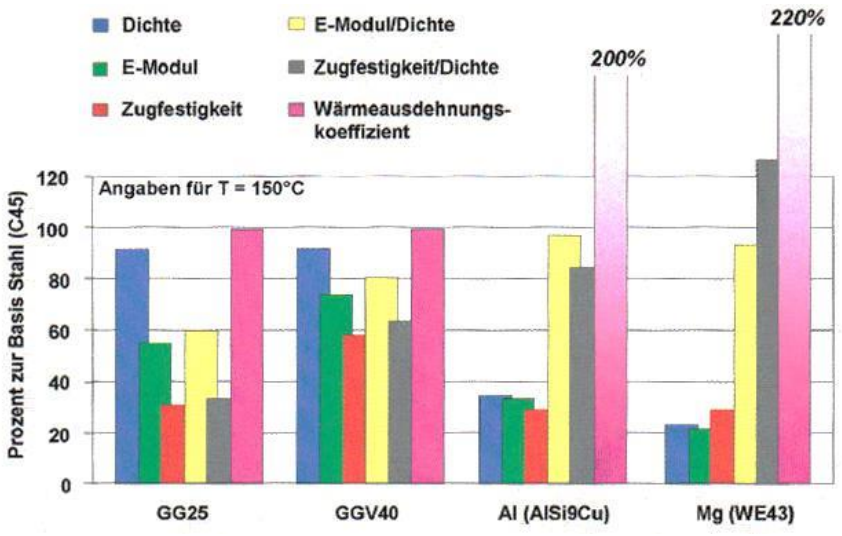

Figure 3 The properties of potential crankcase materials [8]

The advantages of aluminium and magnesium alloys show with regard to the specific weight are notable. However, they are characterized by lesser values of stiffness and strength. Both material groups have good qualities concerning the ratio of Young´s modulus and strength in comparison with mass density, which makes them suitable candidates for lightweight design. Notwithstanding this, they have considerable disadvantages in terms of thermal expansion coefficient. Without counter-measures, the greater thermal expansion would cause unacceptably high bearing clearances during engine operation. These high clearances would drastically increase the oil consumption and worsen the acoustic excitation [8].

While aluminium shows a very good thermal conductivity, the values for magnesium appear on same level as grey cast iron, so that further problems occur with regard to liner deformation and the thermal loads at the inter-bore section. Both light-weight materials necessitate additional measures for the realization of a wear resistant coating for the cylinder liner. Moreover, it has to be taken into account during the design phase that both materials have only a limited creep resistance.

In summary, it can be said that the functional demands on an engine block for high peak pressures usually can be well met by GJL materials. The GJV materials offer still higher degrees of stiffness and strength. The lightweight materials have disadvantages in this respect, but they also have the great benefit of the lower specific weight. The missing wear resistance (cylinder liner) and the high thermal expansion coefficient constitute further challenges for engines made from lightweight alloys. These drawbacks can be compensated by design measures, which cause, however, additional efforts and consequently higher costs.

The different block variants can be further broken down according to their design layout of the cover plate, cylinders and main bearing blocks. For engine blocks aluminium-silicon alloys with Si contents from 6 to 17% and copper contents from 3 to 4% are in use. Secondary alloys, such as ALSi9Cu3, account for the bulk of the casting alloys due to their favourable costs [8].

CYLINDER LINER

The standard solution for the cylinder liner in the aluminium cylinder block is a liner made from cast-iron material. This liner is usually cast into the aluminium. A wall thickness of up to 1.5 or 2 mm can be achieved after machining [2].

The strain on the inter-bore section comes from the superposition of thermal stress due to the temperature profile, and the mechanic stress due to the assembly forces and the cylinder pressure. In the case of high peak pressures especially the dynamic strain increases, so that considerable deformations and stresses occur in the inter-bore section. These can be counteracted by the sufficient dimensioning and the appropriate design of the inter-bore section in combination with efficient cooling. As example for a 2.0 litre four cylinder engine intended for peak pressures of 200 bar, inter-bore section widths of less than 10 mm are difficult to realize with cast iron liners [2,8].

In case of a direct coating of the liner surface (plasma coating technique in mass production) the circumstances are a little more favourable [1,7,7,9,12]. With this method, the space gained for aluminium in the inter-bore section can be used for cooling measures, and minimum inter-bore thickness can be reduced by 1-2 mm. Plasma coatings do not only offer advantages in terms of weight, but also in terms of friction [1,8,12].

An example of a cylinder liner produced by cast-in-spray-compacted aluminium liners is the V12 cylinder engine block used in the Maybach and DaimlerChrysler´s S Class, Figure 4 (a). This engine is unique in that it features the world´s only 12 cylinder crankcase mass-produced by pressure die casting. Moreover, this design consists of the engine block and bedplate [2,10].

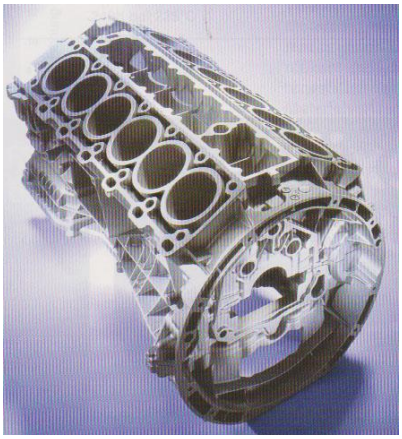

Figure 4 (a) 12-cylinder engine block for the Maybach and the DaimlerChrysler S-Class cast in ALSi9Cu3, block weight including the bedplate; weight approx. 38 kg

(b) 6-cylinder gasoline engine block (DaimlerChrysler) with Silitec® liners

Figure 4 (a) illustrates wear-resistant cylinder liners which consist of a hypereutectic AlSi alloy developed by PEAK Werkstoff GmbH as a lightweight alternative to the considerably heavier cast iron cylinder liners. This is also an alternative to the relatively expensive monolithic engine block made from the hypereutectic primary AlSi17Cu4Mg (Alusil®) casting alloy. The cylinder liners can then be cast-in, preferentially using the high pressure die casting process with a lower cost (secondary) AlSiCu casting alloy [1,8,12].

The Silitec® hypereutectic liner materials are produced by spray compaction; the spray-compacted ingots are subsequently extruded. The high solidification rate of the spray compaction process leads to significantly smaller primary silicon particles than in standard casting processes and ensures excellent tribological properties of the liner surface after the special honing process, Figure 4 (b). Since the same base material is used, metallic bonding between the liner and the engine block is achieved over more than 50% of the contact surface. The result is an engine block showing low distortion and high dimensional stability [1,12].

APPLICATION OF TRIBOLOGICAL METHODS DURING CONSTRUCTION AND PROCESSING OF RECIPROCATING MACHINES

The main parameters which the designers need to know are friction, wear and service life of the machine's parts. The use of ALSi (Alusil®) alloys as a substitution for engine cylinder block made of grey cast iron, in addition to positive aspects such as the lowering of engine weight has also negative tribology side if looking to undesirable properties of this material. According to the later, need to be improved wear resistance of the aluminium alloys to provide their tribology similar to grey cast iron [1].

Today, a wide range of surface coating technologies is available and there are many different wear-resistant materials or material combinations which are applicable for surface coating. Consequently, it exists more of methods have been examined or actually applied for the surface coating of aluminium cylinder liners.

Applying a coating directly to the cylinder surfaces in aluminium machine blocks can eliminate the need for cast iron sleeves. This can significantly reduce the weight of the block; leads to improved heat transfer from the combustion chamber into the water jacket and can give an extra corrosion protection of the running surface. One of existing solutions to overcome undesirable aluminium tribology is the direct coating of cylinder running surfaces with different technologies, among which the application of thermal spray process - plasma coating (Rotaplasma®) (atmospheric plasma spraying - APS) is often used. The whole process of the cylinder surface coating is illustrated schematically in Figure 5 (a) on an aluminium engine block (without washing /cleaning). The process flow is identical for coating of liners that are typically made of cast iron. As indicated above, the APS coatings are applied with a rotating plasma torch designed for machine blocks, Figure 5 (b) [1,12].

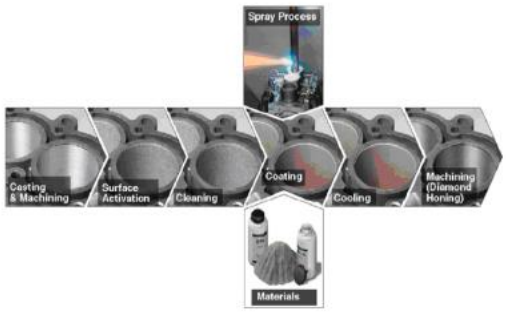

Figure 5 (a) Schematic representation of the SUMEBore coating process (from left to right,

including honing)

(b) F210 plasma torch in an ø81 mm bore of an aluminum engine/ gas compressor block [1,12]

The atmospheric plasma spray process can apply by far the widest variety of coating materials of any thermal spray process. The flexibility of the plasma spray process is based on its ability to develop sufficient energy to melt almost any coating feedstock material in powder form. The feedstock material is injected into the hot plasma plume, where it is melted and propelled towards the target substrate to form the coating [1,12].

The composition of the coatings is dependent of the working conditions, as it is excessive abrasive wear, scuffing, corrosion caused by fuel and gases, intensified heat transfer from the combustion chamber into the water jacket, etc. The coatings must meet the requirements of intensive thermal stresses and wear resistance. Otherwise, the result could be delamination of coating materials and machine failures. Good results were achieved using Fe as a coating material. Furthermore, FeO and Fe3O4 can be dispersed in the layer acting as a solid lubricant such as graphite in grey iron, Figure 6 [9,12]

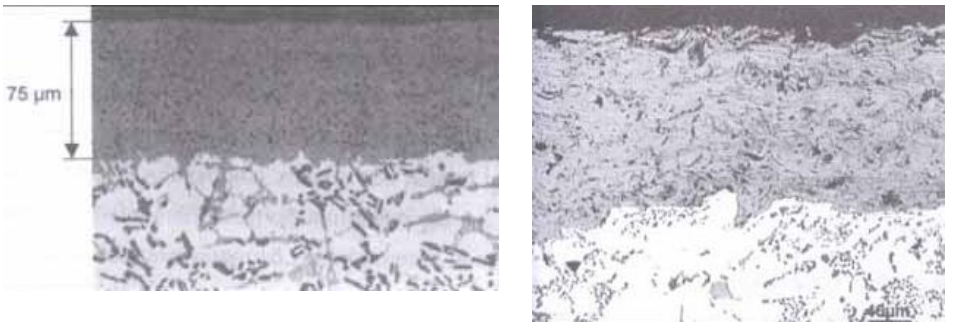

Figure 6 (a) Micrograph showing Ni-SiC dispersion layer (Kolbenschmidt)

(b) Micrograph showing plasma coating layer (Sulzer Metco)

PISTON RINGS COATING – AN EXAMPLE OF TRIBOLOGICAL OPTIMIZATION

Other applicable methods include laser coating of an AlSi alloy, physical (PVD) and chemical vapor deposition (CVD), etc., using materials such as diamond-like carbon (DLC), chromium nitride, titanium nitride, i.e. many different surface coating structures and chemistries [1,4,12].

The piston ring pack as example has a significant potential for bringing down friction losses due to its fairly high (24%) share of mechanical frictional losses in gasoline engines, Figure 7. At the same time measures such as direct injection and turbocharging among others, which increase engine performance, intensify the requirements for the functional behaviour of piston rings [4,11].

When considering measures to optimize the tribology of the system piston ring and cylinder surface, piston ring coatings play an increasingly important role as they can directly influence the wear and friction behaviour and the resulting scuff resistance. By introducing Carboglide Federal-Mogul is providing a coating for piston ring applications which meets

the most stringent requirements for functional behaviour and offers a considerable potential to reduce frictional losses.

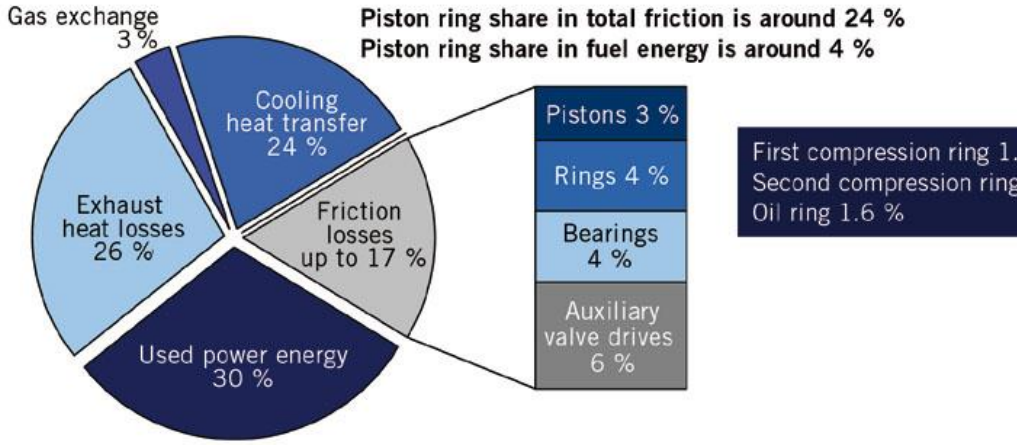

Figure 6 Energy distribution diagram showing friction losses in gasoline engines with the proportionate share of the piston rings [4]

Carbon-based coatings (DLC, Diamond-like Carbon) have a long track record in applications for cutting tools and com¬ponents that are tailored for the most severe tribological requirements [1,12].

The new coating combines extremely low friction values with high strength and durability of piston rings and cylinder running surfaces. By using this coating, the ring pack's frictional losses can be reduced by up to 20%. It significantly protects the cylinder running surface against scoring, increased wear and scuffing during inadequate lubrication. Carboglide makes a substantial contribution to the development of high performance gasoline engines with even better fuel economy by up to 1.5 % with consequently lowering exhaust emissions [4].

Honing of ALSi surfaces

The various cylinder liner manufacturing technologies based on hypereutectic AlSi alloy compositions (Alusil®, Silitecl®, etc.) rely on the presence of a dense distribution of hard, primary silicon particles which act as the tribological partners for piston and piston rings. The technical requirements like low friction, high stability and good lubrication under dry sliding conditions can only be met by the presence of an appropriate surface topography. This structure is created by a special honing process which is different from the conventional honing of grey cast iron. Honing of hypereutectic ALSi surfaces usually requires the following steps [1,9,12]:

- A pre-honing step corrects the cylinder shape and removes most of the damaged surface layer resulting from pre-machining.
- In the following base-honing step, the final surface shape of the primary silicon particles is created.
- Subsequently, a recessing of the aluminum matrix and an exposure of the silicon particles is carried out providing both hard particles to withstand the sliding wear of the piston and to provide oil reservoirs for good distribution of the lubricant. For this

honing step special tools are used with the abrasive particles being smaller than the Si particles and embedded in a soft matrix.

Compared to recessing by etching, this technique provides smooth particle edges which prevent break-outs, Fig. 7.

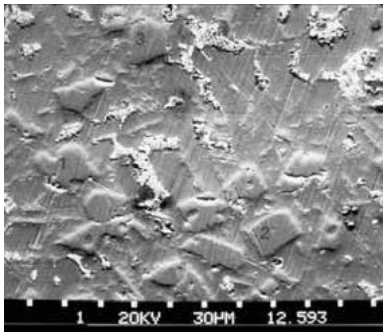

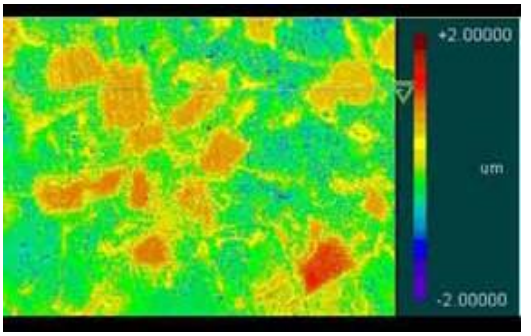

Figure 7 (a) Micrograph showing the final surface after honing with recessed AL matrix and exposed Si particles

(b) Image from white light interference microscope showing the topography of the final cylinder surface

The new concepts piston and cylinder

In order to illustrate some of the concepts discussed above, patented is a small air reciprocating compressor with a 74 mm bore and 35 mm stroke with parts made from aluminium alloys [3,7]. The previous was traditionally made from grey cast iron. The compressor is currently being experimentally investigated on a custom test rig for small air compressors in the Engine Laboratory of the Faculty of Engineering, University of Kragujevac (FINKG) [5,6,7].

Use of AL alloys as a substitution for reciprocating machine blocks made of grey cast iron, has positive aspects in term such as reduction of machine weight etc., as it is described above. But if we looking generally, most aluminium alloys, specifically those suitable for mass production from the technological and economic aspect, do not have satisfactory wear resistance, i.e. their tribological properties are relatively poor. In such cases there is a requirement to improve wear resistance of aluminium alloys, i.e. to provide a least such tribological properties like those of grey cast iron or even better ones. According to this, the surface engineering of the engine cylinder liner is in the focus of most producers of aluminium reciprocating machines [1,7,10,11,12].

According to the latter, as a contribution, patented is the AL cylinder for experimental reciprocating air compressor, coated inside by air plasma spray process (APS). Applied coating materials have good resistance to wear (appropriate steel or cast iron) and good mechanical and tribological properties, Figure 8 [3,7], where the continual tribological pads (2) and/or discrete tribological pads (3) are set into a cylinder (1) in the part over which piston rings slide during operation. These methods are applicable to improve tribological characteristics of AL alloys. The main idea is that relatively small amount of reinforcement can improve characteristics of material by several time. Also, the fact is that tribological properties are the one that define possible application of material, far more than their mechanical properties, since they are in better correlation with behaviour in practice.

However, more measurement data are required before a fully qualified statement as to its general utility can be made. There are a great number of parameters that influence on quality and characteristics of deposited coating.

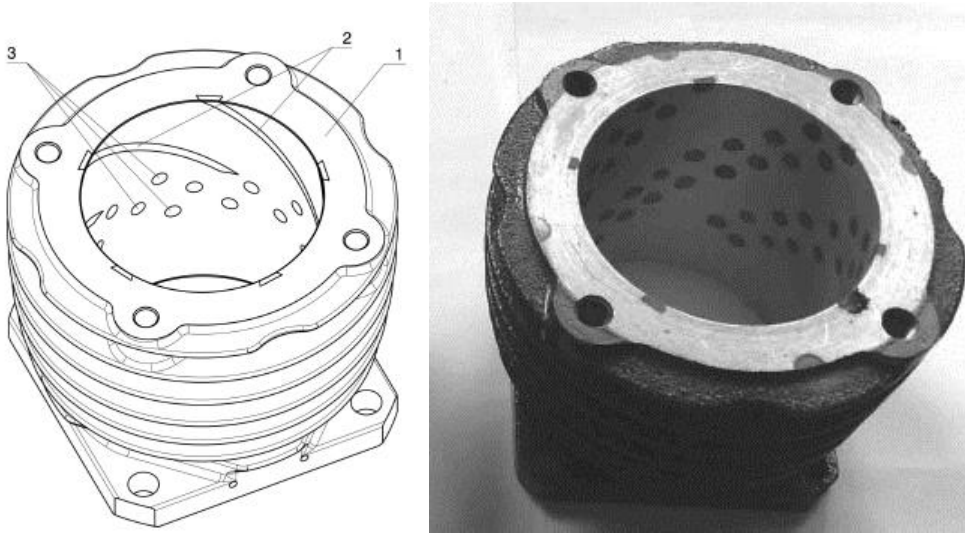

Figure 8 (a) Cross section of patented aluminium cylinder with tribological pads (2-continual and 3-discrete pads)

(b) Single aluminium cylinder that was used as a technology demonstrator at FINKG [2,7]

The main directive of tribological optimization demands the transfer of all limit lubrication cases to hydrodynamic lubrication. In accordance with this request, it is patented the new solution of the pistons with tribological pads for use in reciprocating machines, as example for the use inside of ICEs, Figure 9, as well as for air compressors [7].

The main task of the tribological pads, in the new piston construction, is to reduce friction between the piston and the cylinder, specifically during the engine-starting regime.

Besides that, they transfer piston wear to easily replaceable pads, so in future, the repair of the piston group merely reduces to change of the worn piston rings and pads. The piston becomes only the carrier of the parts that are worn and easily replaceable.

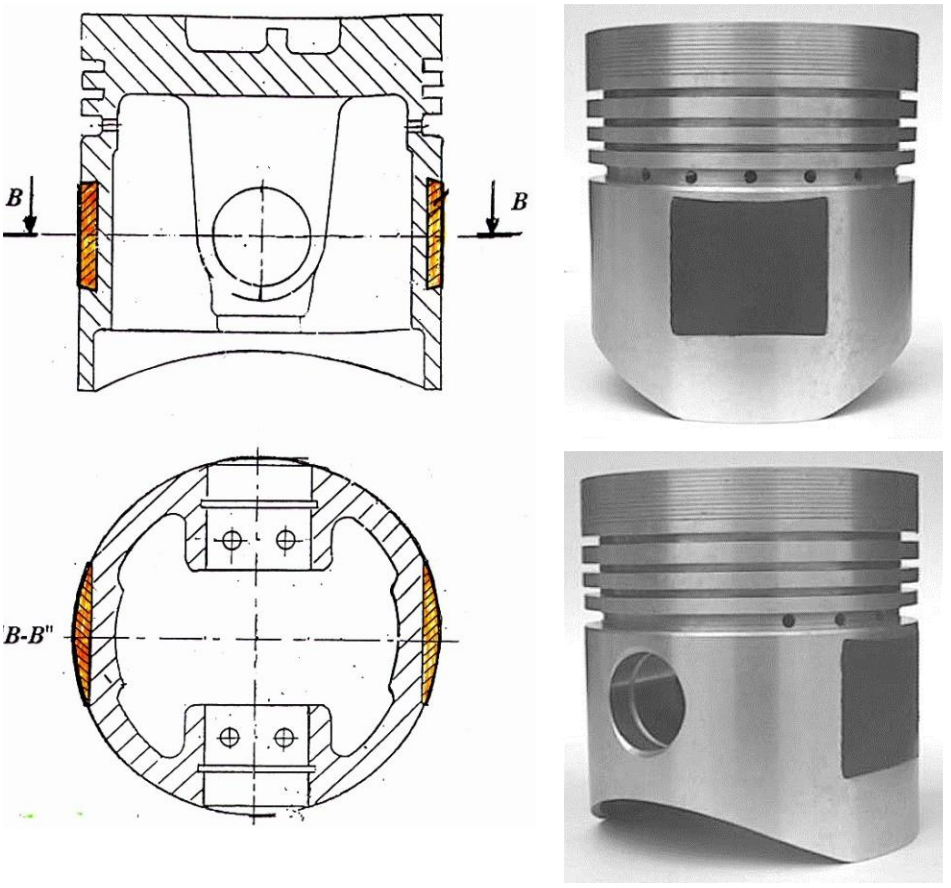

Figure 9 (a) Cross section of patented aluminum piston with tribological pads

(b) Image of new piston design with mounted tribological pads [7]

EXPERIMENTAL INVESTIGATIONS

The first experiments were carried out at the Laboratory for IC engines at the FINK, on a single-cylinder, four-stroke, and air-cooled engine (model No.: 3LD450, Maker: DMB – Lombardini). Main characteristics of the experimental engine are shown in the paper from Pesic et al. [7].

Figure 10 shows the specific work of mechanical losses curves under operation with mounted classic grey cast iron piston as well as with new AL piston with inserted tribological pads, as the the research result of the new piston construction.

The main task of the tribological pads, to reduce friction between the piston and the cylinder is confirmed.

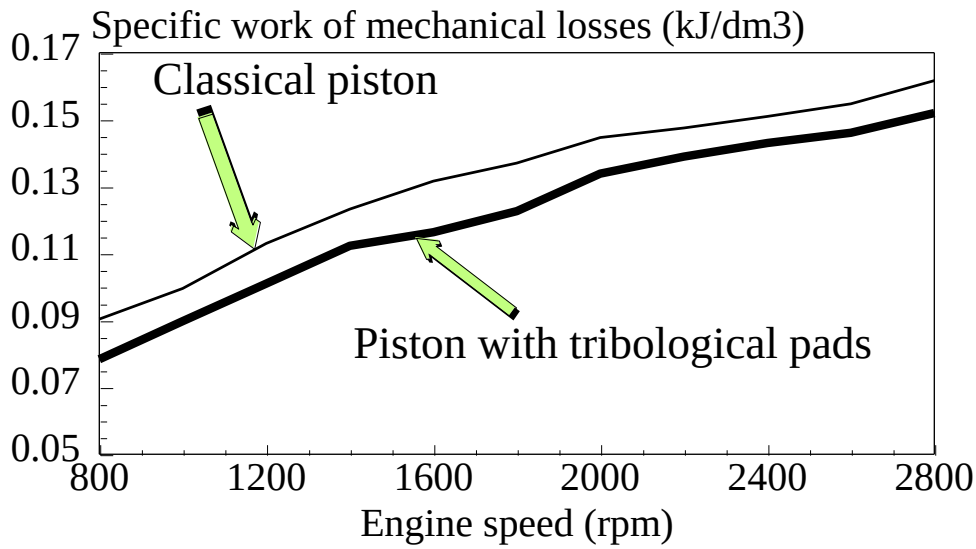

Figure 10 *Specific work of mechanical losses vs. engine speed*

Further researches need to be redirected on the tribological properties under dry sliding conditions, compared with grey cast iron as a standard material for cylinder block an pistons. For the optimized construction of above specified experimental reciprocating air compressor, it is important to significantly reduce lube oil consumption (LOC) towards increasing of machine performance, lowering emission and safe functionality of brake system on the vehicle inside of compressor is used. The latter is important because the presence of lube oil from air reciprocating compressor inside of exhaust (delivery) line on the vehicle can cause the local overheating and air flow restriction, resulting in undesirable malfunction of brake system.

The reduction of the LOC was therefore the prime development goal. The optimization of the system included changes to the piston and piston rings in order to take full advantage of the APS plasma coating, too.

More details about specific machine tests during runs on the test bench and/or in vehicle will be outlined inside of further researches.

CONCLUSIONS

(1) The use of aluminium alloys for substitution of reciprocating machine parts made of grey cast iron has positive effects in term such as reduction of machine weight, but they are characterized by lesser values of stiffness and strength, and their tribological properties are relatively poor.

(2) The greater thermal expansion of aluminium construction would cause unacceptably high clearances during machine operation. These high clearances would drastically increase the oil consumption and worsen the acoustic excitation. In such cases there is a requirement to improve wear resistance of aluminium alloys, i.e. to provide a least such tribological properties like those of grey cast iron or even better ones.

(3) Today, a wide range of surface coating technologies is available and there are many different wear-resistant materials or material combinations which are applicable for surface coating. Consequently, it exists more of methods have been examined or actually

applied for the surface coating of aluminum cylinder liners. Inside of our researches is interesting the atmospheric plasma spray process.

(4) With additional coating on the cylinder liner surfaces it overcoming of poor aluminum strain properties. The application of the piston with tribological inserts towards lowering friction resulting in higher performance of reciprocating machine.

ACKNOWLEDGMENTS

The paper is a result of the research within the project TR 35041 financed by the Ministry of Science and Technological Development of the Republic of Serbia.

REFERENCES

[1] Ernst, P. and Fletcher, K.: SUMEBore – thermally sprayed protective coatings for cylinder liner surfaces. Proceedings of the 6th International MTZ Conference on Heavy-Duty On- and Off-Highway Engines, November 15 - 16, 2011, Kiel, Germany.

[2] Fuchs, H. and Wappelhorst, M.: Leichtmetall-werkstoffe für hochbelastete Motorblöcke und Zylinderköpfe. MTZ Motortechnische Zeitschrift 64 (2003), 10, 868-875.

[3] *Journal: Intellectual Property Gazette.* Pešić, R., Ješić, D. and Veinović, S. 2008. Piston compressors and IC engines cylinder with inserted tribological inserts. The Intellectual Property Office of the Republic of Serbia, Belgrade, 2008/3, pp.598-599.

[4] Kennedy, M., Hoppe, S. and Esser, J. Piston ring coating reduces gasoline engine friction. MTZ Motortechnische Zeitschrift 73 (2012), 5, 40-43.

[5] Milojević S., Pešić R., Taranović D., Davinić A. (2013). MERENJE HODA PLOČE VENTILA EKSPERIMENTALNOG KLIPNOG KOMPRESORA, Journal Tractors and Power Machines, Novi Sad, ISSN 0354-9496(2012) 17: 2/3, p. 71-77, UDK 621.629.

[6] Ninković, D., Taranović, D., Milojević, S. and Pešić, R. (2012). Modelling valve dynamics and flow in reciprocating compressors – a survey. International Congress Motor Vehicles & Motors 2012, Kragujevac, October 3 - 5, 2012, Proceedings (Pešić R., Lukić J.), MVM2012-022, pp. 113-125, ISBN 978-86-86663-91-7.

[7] Pešić, R. (2004). ASMATA – Automobile Steel Material Parts Substitution with Aluminium. Int. J. Vehicle Mech., Engines and Transportation Syst. Special Edition, 30, 1-168 (In Serbian and English).

[8] Schwaderlapp, M., Bick, W., Duesmann, M. and Kauth, J.: 200 bar Spitzendruck Leichtbaulösungen für zukünftige Dieselmotorblöcke. MTZ Motortechnische Zeitschrift 65 (2004), 2, 84-90.

[9] Vencl, A., Avramović, S., Marinković, A.: Ferrous-based coating deposited on al-alloy substrate by Atmospheric Plasma Spraying (APS), 31. Conference on production engineering with foreign participants, Kragujevac, 19-21.09.2006.

[10] www.federalmogul.com, accessed on August 18th 2014.

[11] www.ricardo.com, accessed on August 18th 2014.

[12] www.sulzer.com, accessed on August 18th 2014.

EXPERIMENTAL EVALUATION OF MAGNETORHEOLOGICAL DISK BRAKE

Aleksandar Poznić [1], *Danijela Miloradović*

UDC: 62.592.35

ABSTRACT: This paper presents experimental evaluation on overall braking capacity of magnetorheological disk brake at various control currents and shaft angular velocity. A magnetorheological brake consists of a rotating disk(s) that is immersed in magnetorheological fluid where the fluid behaviour is changing under influence of magnetic field. The magnetorheological brake was designed in such way that it can be fitted with one or two disks, optionally. The experiments were performed using specially designed test rig to obtain friction, viscous and induced braking torque values in one or two disks configuration. Amplification factor is used to present total braking torque.

KEY WORDS: Magnetorheological disk brake, magnetorheological fluid, test rig, torque, control current

REZULTATI ISTRAŽIVANJA U OBLASTI PRIMENE KOMPOZITNIH I ADHEZIVNIH MATERIJALA KOD LAKIH KONSTRIKCIJA VOZILA

REZIME: U radu je prikazana eksperimentalna ocena ukupnog kapaciteta magnetoreoloških disk kočnica pri različitim jačinama struja upravljanja i ugonim brzinama vratila. Magnetoreološka kočnica sastoji se od rotirajućeg(ih) diska (ova) koja je uronjena u magnetorheološku tečnost tečnosti pri čemu se ponašanje fluida menja pod dejstvom magnetnog polja. Magnetoreološka kočnica je projektovana tako da se može imati jedan ili dva diska, opciono. Eksperimenti su izvedeni korišćenjem specijalno projektovanog mernog mosta za određivanje trenja, viskoznih i indukovanih kočnih momenata kod konfiguracija sa jednim ili dva diska. Za predstavljanje ukupnog kočnog momenta korišćen je faktor pojačanja.

KLJUČNE REČI: Magnetoreološke disk kočnice, Magnetoreološki fluid, merni most, moment, struja upravljanja

[1] *Received: September 2014, Accepted October 2014, Available on line December 2015*

Intentionally blank

EXPERIMENTAL EVALUATION OF MAGNETORHEOLOGICAL DISK BRAKE

Aleksandar Poznić [1], Assistant, Danijela Miloradović [2], PhD, Assistant professor

UDC: 62.592.35

INTRODUCTION

The convectional friction brake (FB) is the most commonly used brake type in almost any mechanical system today. However, it is characterized by drawbacks such as periodic replacement due to wear, large mechanical time-delay, bulky size, etc. [29, 13]. Electromechanical brakes (EMBs) have potential to overcome some of these drawbacks and are a suitable FB replacement. Today, EMBs are applicable in almost any mechanical system. Application of intelligent materials is the next step in EMB's development.

Magnetorheological fluids (MR fluids) belong to a class of intelligent materials that respond to applied magnetic field with fast, continuous and reversible change in their rheological behaviour [7, 28, 3]. MR fluids are type of suspensions. Carrier fluid is usually mineral or synthetic oil, water, kerosene etc. with dispersed micro size ferromagnetic particles. When exposed to external magnetic field, particles form a chain-like structures thus changing fluid's viscosity. In this research, authors used BASF's MR fluid "Basonetic 5030".

MR fluids have attracted extensive research interest in recent years since they can provide simple, quiet and fast response interface between electronic control and mechanical system [22, 20, 11]. A lot of work was done on MR fluid brakes modelling, properties investigation and control [6, 11, 3]. A wide range of MR fluid devices have also been investigated for their potential applications in different systems, such as: clutch systems, vibration control, seismic response reduction, etc. [9, 10, 26].

MR fluid brakes have also been used in actuators due to their distinguished force control and power transmission features [5, 15]. By applying a proper control effort, viscosity with large varying range is achievable with the MR fluid brake. Currently, there are many solutions for MR fluid brake design. Some MR fluid brakes with attractive properties, such as high yield stress and stable behaviour, have been developed and commercialized [16, 4].

The objective of this work was to evaluate overall braking torque for experimental MR fluid brake model. Based on literature research [1] and earlier authors' works, MR disk brake was manufactured and tested on a specially designed test rig. Results were presented as amplification factors and discussed latter on.

MAGNETORHEOLOGICAL EFFECT

MR fluids are suspensions composed out of three major components: carrier fluid - usually mineral or synthetic oil, magnetizable particles - carbonyl iron powder and set of additives [17, 2]. When exposed to an external magnetic field (ON state), change in MR

1 Aleksandar Poznić, M. Sc., assistant, University of Novi Sad, Faculty of Technical Sciences, 6 Dositeja Obradovića Square, Novi Sad, Serbia, alpoznic@uns.ac.rs
2 Danijela Miloradović, Ph. D., assist. prof., University of Kragujevac, Faculty of Engineering, 6 Sestre Janjić Str., Kragujevac, Serbia, neja@kg.ac.rs

fluid's viscosity occurs. In the absence of an external magnetic field (OFF state), MR fluid acts as Newtonian fluid [7,11] and can be described as:

$$\tau = \eta \cdot \dot{\gamma} \tag{1}$$

where: τ represents shear stress, η - fluid`s viscosity and $\dot{\gamma}$ - shear rate, often, for MR fluid brakes, denoted as $\dot{\gamma} = \frac{r\omega}{g}$, where *r* is rotor radius, ω and *g* are angular speed and MR fluid gap length, respectively.

When in ON state, MR fluid's rheological properties do change. Magnetizable particles induce polarization and form chain-like structures in magnetic flux path direction, thus changing apparent viscosity of the fluid. ON state behaviour of MR fluid is often represented as a non-Newtonian [1, 5, 3], having a variable yield strength. The usage of Bingham's model (2), in this situation, gives reasonably good results [22, 1, 20, 11]:

$$\tau = \tau_{\mathrm{B}} + \eta \cdot \dot{\gamma} \tag{2}$$

where: τ_{B} is the yield stress, developed in response to the applied magnetic field. Its value is a function of the magnetic field induction, *B*.

When used in a device, MR fluid can be in one of four modes: Shear, Flow (Pressure), Squeeze and Pinch, [8, 18, 28]. In brake i.e. torque transfer applications, MR fluid operates in Shear mode [1]. Braking torque values are adjusted continuously by changing the external magnetic field strength.

MAGNETORHEOLOGICAL BRAKES

MR brake consists of four main parts: rotor, housing (stator), coil and MR fluid, Figure 1. The rotor's shape is what differentiates MR brake types from each other. One needs MR brake's quantitative parameters, to be able to determine its specific application suitability.

Magnetorheological brake types

Through literature research [22, 24, 9, 14, 23], authors of this paper have identified five major MR fluid brake designs: drum brake, inverted drum brake, disk brake, T-shape rotor brake and multiple disks brake, Figure 1.

Drum brake along with the disk brake is the easiest designs to manufacture. However, large inertia is its major drawback compared to disk brake design [1].

The disk brake design is the most common MR brake design found in literature today and was the first one to be investigated [25]. It is the easiest one to manufacture and gives reasonably good results in terms of weight and compactness [14]. There are some variations in MR disk brake design such as: the use of two coils instead of one in order to increase the magnetic pole area and/or relocation of the coil on top of the disk in order to reduce its external diameter [22], but the basics remain the same. It is also interesting to note that the MR disk brake design is currently the only one commercially available as a standard product, manufactured by Lord Corporation [16] and that it was used in several studies [7, 21, 19].

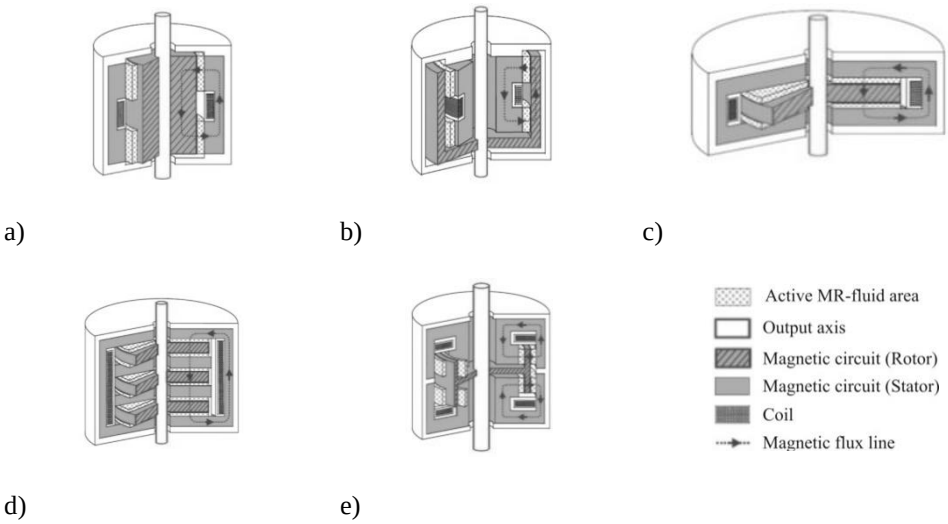

Figure 1 Types of MR brakes, a) drum, b) inverted drum,

c) disk, d) multiple disks, e) T-shaped rotor [29]

In order to increase compactness of the MR disk brake design, several disk-shape rotors can be used instead of one, with segments of stator located between each rotor disk, Figure 3, d). This multiple disk design is very popular in literature and was used in several applications that required high torque in limited space and weight [22, 13, 23]. The equations describing this particular design are very similar to those of the single disk brake.

The T-shape rotor brake design, Figure 1, e), is more compact than all other designs, but it is also more complex to manufacture. Despite its advantages, this design is not so common in literature [22].

For all aforementioned MR brake types, the rotor has a cylindrical shape and the magnetic flux lines run in the radial direction, Figure 1.

To authors' knowledge, an in-depth comparison of all these architectures is not yet available.

Mechanical model

The key objective in MR fluid brake design is to establish the relationship between the overall braking torque, magnetic field strength and design parameters. Change in MR fluids viscosity and its interaction with the inner surfaces of the brake will generate the overall braking torque. Based on Equation (2) and MR brake's specific geometrical configuration, for all MR brake types, it applies:

$$dT = 2\pi N \tau r^2 dr \tag{3}$$

Where: N is number of surfaces of the rotor, perpendicular to the magnetic flux lines and in contact with MR fluid and r is the rotor's radius.

The overall braking torque, $T_{Overall}$, consists of three components:

- the magnetic field induced component, T_B, due to the field-dependent yield stress,

- the fluid viscosity dependent component, T_{vis}. and
- the friction induced component, T_{fric}

Thus, the overall brake torque is:

$$T_{Overall} = T_B + T_{vis} + T_{fric} \tag{4}$$

The sum of the first two components, T_B and T_{vis}, i.e. the braking torque, can be obtained by the following integral:

$$T_B + T_{vis} = 2\pi N \int_{R_i}^{R_o} \tau r^2 dr \tag{5}$$

where: R_o and R_i are the brake's rotor outer and inner radii, respectively. Considering practical conditions, for all MR brake types, the value of the R_i can be ignored, because R_o is several order of magnitude of R_i. The final MR disk brake overall braking torque expression is:

$$T_{overall} = T_B + T_{vis} + T_{fric} = \frac{4}{3}\pi\tau_B R_o^3 N_d + \pi\eta\frac{\omega}{g}R_o N_d + T_{fric} \tag{6}$$

where: N_d, ω, g are number of disks in use, angular speed and MR fluid's gap, respectively.

Aspect of commercial availability of materials was considered, so authors decided to use AISI 1018 chemical equivalent, Č1221. The $B-H$ curves for Č1221 and Basonetic 5030 are presented in Figure 2. The first step in deterring the MR brake's analytical braking capacities was to determine the operating point couples for materials in use. The higher values were preferable but also require larger coil. Two coils were manufactured for this experimental purpose, with 250 and 500 coils.

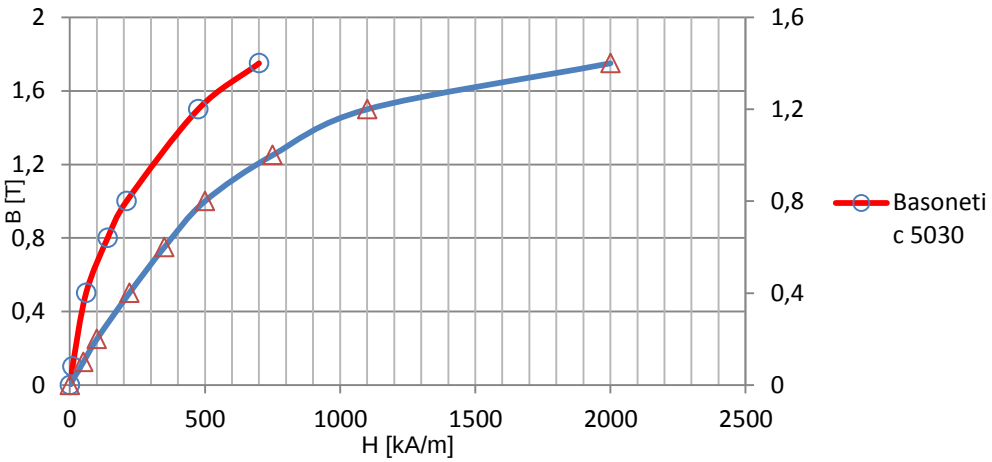

Figure 2 B-H curves for Basonetic 5030 and AISI 1018

In this configuration, magnetic field induction was low and around 0.1 T, placing material's operating points at the very root of $B-H$ curves. This low value magnetic field produced low value shear stress in the MR fluid. Placing above mentioned brake's

characteristic and fluid's ON and OFF values in Equation 6, estimated overall braking torque was around 0.2 Nm

Test rig

Based on test rigs literature research [10, 27, 20, 15], the authors of this paper selected the most promising MR brake test rig design and manufactured it. With lowest inertia, good dynamic range and the highest mechanical simplicity, the disk type promised the biggest potential.

The test rig was designed and manufactured at Faculty of technical sciences, Novi Sad, Serbia, and is presently at its Laboratory for engines and vehicles. The test rig with its parts is depicted in Figures 3 and 4, and consists of four main parts:

- drive,
- power supply,
- MR brake and
- measurement and data acquisition equipment.

An 8-pole AC motor, 5 AZ 100 LA – 8 model (*Koncar*), with power of 0.75 kW and maximum speed of 750 rpm, Figure 3, position 2, was placed at one end of the support-frame of the test rig. The inverter –VLT 5400 (*Danfoss*), Figure 3, position 1, controls the AC motor's direction and variable-speed. Speed was changed with increment of 50 rpm, in a range from 50 rpm to 700 rpm. These two elements form a drive part of the test rig. The flexible coupling, Figure 3, position 3, connects AC motor and the MR brake's shaft. MR brake rests on two self-aligning ball bearings, 6000 (*Fag*). To avoid leakage of MR fluid, Nitrile Rubber lip seals, suitable for MR type application, have been used.

Torque transfer from the MR brake to a measurement device was done indirectly. A load arm, connected to the MR brake housing at one end, rests on top of the load cell on the other end, Figure 3. Thus, by measuring the force on the load cell, the value of transmitted torque was obtained. Load cell was internally calibrated by calibration weights. The capacity of the load cell, PW6CC3MR (*HBM*), was 7 kg.

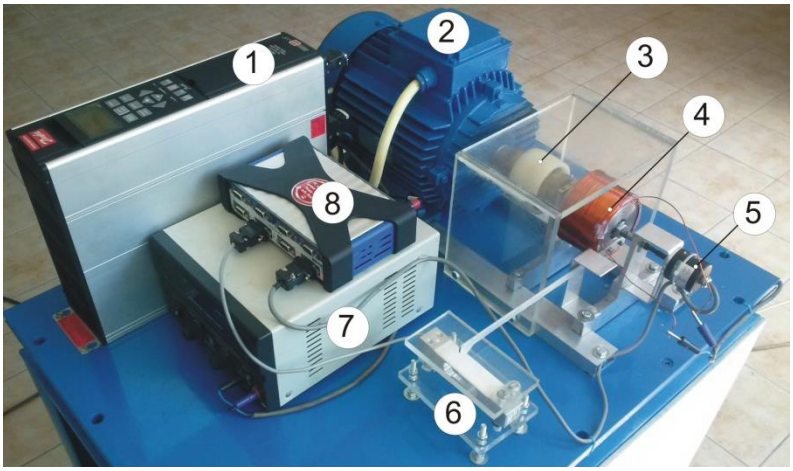

Figure 3.Test rig for magnetorheological brake performance evaluating:

1. inverter, 2. AC motor, 3.coupling, 4. MR fluid brake, 5. optical encoder, 6. load cell, 7. DC power supply,8. data acquisition card

The optical encoder, model AMT102-V-REV-C (*CUI Inc.*), was connected to the MR brake's shaft, at the opposite side of the AC motor and rotated at the same speed. Sample rate was 2048 per rotation. The signals were processed by data acquisition card, Quantum MX840A *(HBM)*, Figure 4, position 8. The DC power supply, EA PS 2016-100 (*Elektro-automatik*), was connected to the leads of the coil to provide flux generation. This was the control current, with range of 0 A to 5 A or 10 A, depending on coil configuration. Increment was 0.2 A. The coil, made of copper wire with diameter of 1 mm (18 gauges) has been coiled on outer radius of the MR brake housing, ϕ 73 mm.

The MR fluid used in this experiment was Basonetic® 5030, from BASF® [17]. It is a carbonyl iron powder based MR fluid.

A typical testing procedure was as follows. Firstly, the MR brake's shaft was set to a certain speed for 1 min as an initial condition, which stirred the MR fluid in the brake to distribute it uniformly. The desired magnetic field was then applied by setting the coil current (control current) and waiting for 1 min. This ensured the forming of MR fluid's stable structure. The load cell detected transmitted torque. Finally, the signal from the load cell was processed and recorded.

EXPERIMENTAL RESULTS

The goal of this experiment was to determine overall braking torque capabilities of the selected MR brake design. The experiment was conducted on a specially designed test rig, with different control currents and speed sets. To eliminate the effects of previous observations, different combinations of control current and rotational speed were set for each reading. To bring repeatability in the reading, every speed set was carried out twice at different instance of time. For every reading, before torque data recording, approximately 1 min time has been allotted to uniformly distribute the carbonyl iron particles in the MR fluid and form a stable structure.

The experiment consisted out of tree parts. The first part was to determine the influence of the supporting ball bearings and seals, without MR fluid inside the brake and no control current applied. This was a friction component of braking torque. The second part of the experiment had the same setup, but it included MR fluid inside the brake. Viscous torque data was then recorded, assuming that bearings and seals did not change their friction characteristics in time.

Aforementioned recordings were needed in order to get clear and precise information about field induced component. This was the third part of the experiment and it included MR fluid inside the brake and application of the control current.

The same speed sets that were used for measurements of the friction and the viscous torque components were repeated. For each speed set, there was a 2 minutes recording time. Some field induced component results are presented in Figure 4. Magnetic field influence is apparent.

Because of the large quantity of data obtained in this experiment, authors decided to use amplification factor to determine the effect produced by magnetic field. Amplification factor represents relation between overall braking torque and sum of friction and viscous torque, i.e. relation between the MR fluid's ON and OFF state:

$$\text{Amplification factor} = \frac{T_{Overall} \text{ at current I}}{T_{Overall} \text{ at zero current}} \quad (7)$$

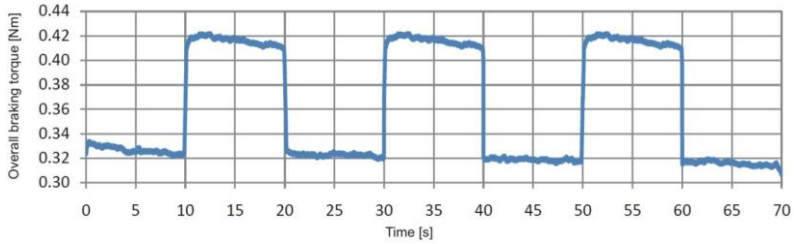

Figure 4 Sample of overall braking torque results

Amplification factor curves for all 14 speed sets are plotted in Figure 5. This figure shows linearity in amplification factor with increase in control current. This was expected, since the higher the current, the higher the field induced torque should be. Results are presented with rotational speed variation as well.

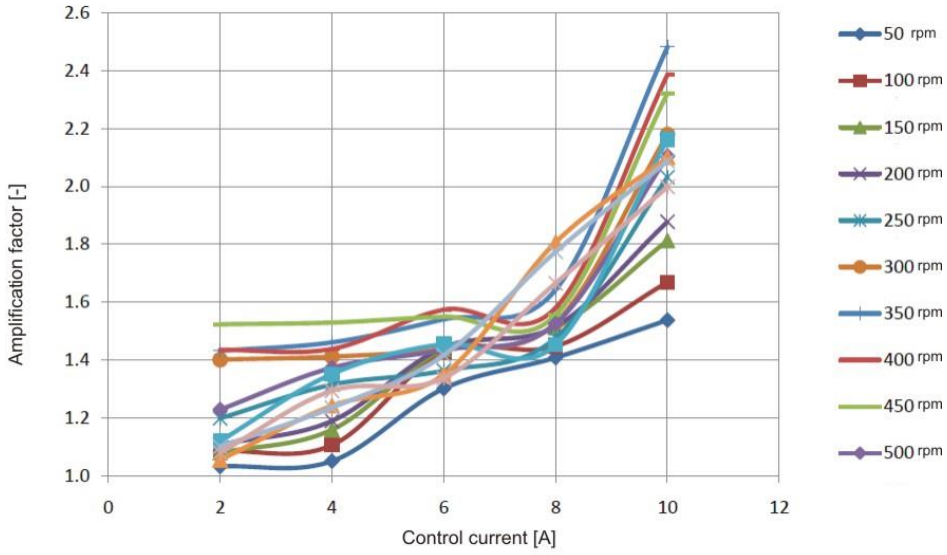

Figure 5 Variation in amplification factor with control current

Transition control current value for this MR brake model was 8 A. This was somewhat opposite to the torque predicted by equation (6) where $T_{Overall}$ should increase more linearly with control current. This was not the case here. However, other authors have also reported the same trend - reduction of amplification factor with increment of speed and control current [27, 20]. This may be due to the possible shear thinning effect of the MR fluid at high shear rates. This reduces the effectiveness of MR brake at higher speeds. Therefore, to make MR brake effective at higher speed operation, one needs to think of „shear stable MR fluid".

CONCLUSIONS

Based on literature research, the authors have decided for the most promising MR brake type, manufactured it and tested it on a specially designed test rig.

The MR brake produced desirable response and predicted results, which coincide with literature sources. Approximately linear relation between the overall braking torque and the control current intensity was observed. To present results in more readable manner, the amplification factor was introduced.

The experiments have shown that the tested MR brake has potential for practical applications due to easiness and accuracy of control. However, the value of the overall braking torque is still small. To increase it, better utilization of the existing magnetic field is needed. The authors suggested different approach in comparison to the conventional MR brake design that would increase the overall braking torque by increasing the magnetic field efficiency and MR brake's fluid contact area. By multiplying the number of the disks in contact with MR fluid, value of the overall braking torque will multiply as well, Equation (6).

In order to maximize proposed MR brake's potential, further investigations on magnetic field propagation are needed as well as design optimization. Finite element method model of the novel MR brake is the next step in this process.

ACKNOWLEDGMENTS

This research was done as a part of the project TR31046, "Improvement of the quality of tractors and mobile systems with the aim of increasing competitiveness and preserving soil and environment", supported by Serbian Ministry of Science and Technological Development.

MR fluid used in this experiment was provided by BASF® Company, under commercial name "Basonetic® 5030". The authors of this paper would like to express their sincere gratitude to BASF Company as well as to project manager Dr. Christoffer Kieburg for all support.

REFERENCES

[1] Avraam, T. M.: MR-fluid brake design and its application to a portable muscular rehabilitation device, PhD thesis, Active Structures Laboratory, Department of Mechanical Engineering and Robotics, Universit´eLibre de Bruxelles, Bruxelles, 2009

[2] Bossis, G., Lacis, S., Meunier, A. and Volkova, O.: Magnetorheological fluids, Journal of magnetism and magnetic materials, Vol. 252, pp. 224-228, 2002

[3] Carlson, J.D. and Jolly, M.R.: MR fluid, foam and elastomer devices, Mechatronics, Vol. 10, pp. 555–569, 2000

[4] Carlson, J.D., Catanzarite, D.M. and Clair, K.A.: Commercial magnetorheological fluid devices. In Proceedings of the 5th International Conference on ER Fluids, MR Suspensions and Associated Technology (Ed. W. A. Bullogh), Singapore, pp. 20–28. 1996

[5] Ericksen, E.O. and Gordaninejad, F.: A magneto-rheological fluid shock absorber for an off-road motorcycle, International J. Vehicle Design, Vol. 33 No 1-3, pp. 139-152, 2003

[6] Farjoud, A., Vahdati, N. and Fah, Y.F.: Mathematical model of drum-type MR brake using Hershel-Bulkley shear model, Journal of Intelligent Material Systems and Structures, Vol. 00, pp. 1–8, 2007

[7] Fernando, D.G.: Characterizing the behavior of magnetorheological fluids at high velocities and high shear rates, PhD thesis, Faculty of the Virginia Polytechnic Institute and state University, Blacksburg, Virginia, 2005

[8] Goncalves, F.D. and Carlson, J.D.*:* An alternate operation mode for MR fluids—Magnetic Gradient Pinch, Journal of Physics: Conference Series, Vol. 149, pp.1–4, 2009

[9] Gudmundsson, K.H., Jonsdottir, F. and Thorsteinsson, F.: A geometrical optimization of a magneto-rheological rotary brake in a prosthetic knee, Smart Materials and Structures, Vol. 19, pp. 1–11, 2010

[10] Herold, Z., Libl, D. and Deur, J.: Design and testing of an experimental magnetorheological fluid clutch, Strojarstvo, Vol. 52, No. 3, pp. 601–614, 2010

[11] Huang, J., Yhang, J.Q., Yang, Y. and Wei, Y.Q.: Analysis and design of a cylindrical magneto-rheological fluid brake, Journal of Material Processing Technology, Vol. 129, pp. 559–562, 2002

[12] Jinung, A. and Dong-Soo, K.: Modelling of magnetorheological actuator including magnetic hysteresis, Journal of Intelligent Material Systems and Structures, Vol. 14, pp. 541-550, 2003

[13] Karakoc, K., Park, J.E and Suleman A.: Design considerations for an automotive magnetorheological brake, Mechatronics, Vol. 18, No. 8, pp. 434-447, 2008

[14] Karakoc, K.: *Design* of a Magnetorheological Brake System Based on Magnetic Circuit Optimization, PhD Thesis, Department of Mechanical Engineering, University of Victoria, Victoria, Canada, 2007

[15] Kavlicoglu B.M., Gordaninejad, F., Evrensel, C.A., Cobanoglu, N., Lui, Y., Fuchs, A. and Korol G.: A high-torque magneto-rheological fluid clutch, Proceedings of SPIE Conference on smart materials and structures, March 2002, San Diego, pp. 1-8

[16] Kayler K.: Lord corporation expands production of steer-by-wire TFD brakes to meet demand, available from: http://www.lord.com/news-center/press-releases/lord-corporation-expands-production-of-steer-by-wire-tfd-brakes-to-meet-demand-.xml. Accessed on June 20th, 2013

[17] Kieburg, C., MR-fluid Basonetic 5030, Technical Information, BASF SE Metall Systems, Ludwingshafen, Germany, 2010

[18] Lange, U., Richter, L. and Zipser, L.: Flow of magnetorheological fluids, Journal of Intelligent Material Systems and Structures, Vol. 12, pp. 161-164, 2001

[19] Lampe, D. and Grundmann R.: Transitional and solid state behaviour of a magnetorheological clutch. In Proceedings of Actuator 2000, Bremen, 2000

[20] Li, W.H. and Du, H.: Design and experimental evaluation of a magnetorheological brake, The International Journal of Advanced Manufacturing Technology, Vol. 21, pp. 508–515, 2003

[21] Liu, B., Li, W.H., Kosasih, P.B. and Zhang, X.Z.: Development of an MR-brake-based haptic device, Smart Materials and Structures, Vol. 15, pp. 1960-1966, 2003

[22] Nguyen, Q.H. and Choi, S.B.: Selection of magnetorheological brake types via optimal design considering maximum torque and constrained volume, Smart Materials and Structures, Vol. 21, pp. 1–12, 2012

[23] Park, E. J., Stoikov, D., da Luz, L. F. and Suleman, A.: A performance evaluation of an automotive magnetorheological brake design with a sliding mode controller, Mechatronics, Vol. 16, pp. 405–416, 2006

[24] Phuong-Bac, N., and Seung-Bok C.: A new approach to magnetic circuit analysis and its application to the optimal design of a bi-directional magnetorheological brake, Smart Materials and Structures, Vol. 20, pp. 1 – 12, 2011

[25] Rabinow, J.: Magnetic fluid torque and force transmitting device. US patent 2,575,360, 1951

[26] Spencer B.F., Dyke, S.J., Sain, M.K. and Carlson J.D.: Phenomenological model of a magnetorheological damper, ASCE Journal of Engineering Mechanics , Vol. 123, No. 3, pp. 1–23, 1996

[27] Sukhwani, V., K. and Hirani, H.: Design, development, and performance evaluation of high-speed magnetorheological brakes, Proceedings of the Institution of Mechanical Engineers, Part L: Journal of Materials Design and Applications, Vol. 222, pp. 73-82, 2008

[28] Wang, J. and Meng, G.: Magnetorheological fluid devices: principles, characteristics and applications in mechanical engineering, Proceedings of Institution of Mechanical Engineers – Part L – Journal of Materials: Design and Application, Vol. 215, pp. 165-174, 2001

[29] Zainordin, Z.A., Abdullah, A.M. and Hudha, K.: Experimental evaluations on braking responses of magnetorheological brake, International journal of mining, metallurgy & mechanical engineering, Vol. 1, No. 3, pp. 195-199, 2013

MVM – International Journal for Vehicle Mechanics, Engines and Transportation Systems

NOTIFICATION TO AUTHORS

The Journal MVM publishes original papers which have not been previously published in other journals. This is responsibility of the author. The authors agree that the copyright for their article is transferred to the publisher when the article is accepted for publication.

The language of the Journal is English.

Journal ***Mobility & Vehicles Mechanics*** is at the SSCI list.

All submitted manuscripts will be reviewed. Entire correspondence will be performed with the first-named author.

Authors will be notified of acceptance of their manuscripts, if their manuscripts are adopted.

INSTRUCTIONS TO AUTHORS AS REGARDS THE TECHNICAL ARRANGEMENTS OF MANUSCRIPTS:

Abstract is a separate Word document, "*First author family name_ABSTRACT.doc*". Native authors should write the abstract in both languages (Serbian and English). The abstracts of foreign authors will be translated in Serbian.

This document should include the following: 1) author's name, affiliation and title, the first named author's address and e-mail – for correspondence, 2) working title of the paper, 3) abstract containing no more then 100 words, 4) abstract containing no more than 5 key words.

The manuscript is the separate file, „*First author family name_Paper.doc*" which includes appendices and figures involved within the text. At the end of the paper, a reference list and eventual acknowledgements should be given. References to published literature should be quoted in the text brackets and grouped together at the end of the paper in numerical order.

Paper size: Max 16 pages of B5 format, excluding abstract
Text processor: Microsoft Word
Margins: left/right: mirror margin, inside: 2.5 cm, outside: 2 cm, top: 2.5 cm, bottom: 2 cm
Font: Times New Roman, 10 pt
Paper title: Uppercase, bold, 11 pt
Chapter title: Uppercase, bold, 10 pt
Subchapter title: Lowercase, bold, 10 pt
Table and chart width: max 125 mm
Figure and table title: Figure _ (Table _): Times New Roman, italic 10 pt

Manuscript submission: application should be sent to the following e-mail:

mvm@kg.ac.rs ; lukicj@kg.ac.rs
or posted to address of the Journal:
University of Kragujevac – Faculty of Engineering
International Journal M V M
Sestre Janjić 6, 34000 Kragujevac, Serbia

The Journal editorial board will send to the first-named author a copy of the Journal offprint.

MVM – International Journal for Vehicle Mechanics, Engines and Transportation Systems

OBAVEŠTENJE AUTORIMA

Časopis MVM objavljuje orginalne radove koji nisu prethodno objavljivani u drugim časopisima, što je odgovornost autora. Za rad koji je prihvaćen za štampu, prava umnožavanja pripadaju izdavaču.

Časopis se izdaje na engleskom jeziku.

Časopis ***Mobility & Vehicles Mechanics*** se nalazi na SSCI listi.

Svi prispeli radovi se recenziraju. Sva komunikacija se obavlja sa prvim autorom.

UPUTSTVO AUTORIMA ZA TEHNIČKU PRIPREMU RADOVA

Rezime je poseban Word dokument, "*First author family name_ABSTRACT.doc*". Za domaće autore je dvojezičan (srpski i engleski). Inostranim autorima rezime se prevodi na srpski jezik. Ovaj dokument treba da sadrži: 1) ime autora, zanimanje i zvanje, adresu prvog autora preko koje se obavlja sva potrebna korespondencija; 2) naslov rada; 3) kratak sažetak, do 100 reči, 4) do 5 ključnih reči.

Rad je poseban fajl, „*First author family name_Paper.doc*" koji sadrži priloge i slike uključene u tekst. Na kraju rada nalazi se spisak literature i eventualno zahvalnost. Numeraciju korišćenih referenci treba navesti u srednjim zagradama i grupisati ih na kraju rada po rastućem redosledu.

Dužina rada: Najviše 16 stranica B5 formata, ne uključujući rezime
Tekst procesor: Microsoft Word
Margine: levo/desno: mirror margine; unurašnja: 2.5 cm; spoljna: 2 cm, gore: 2.5 cm, dole: 2 cm
Font: Times New Roman, 10 pt
Naslov rada: Velika slova, bold, 11 pt
Naslov poglavlja: Velika slova, bold, 10 pt
Naslov potpoglavlja: Mala slova, bold, 10 pt
Širina tabela,dijagrama: max 125 mm
Nazivi slika, tabela: Figure __ (Table _): Times New Roman, italic 10 pt

Dostavljanje rada elektronski na E-mail: **mvm@kg.ac.rs ; lukicj@kg.ac.rs**

ili poštom na adresu Časopisa
Redakcija časopisa M V M
Fakultet inženjerskih nauka
Sestre Janjić 6, 34000 Kragujevac, Srbija

Po objavljivanju rada, Redakcija časopisa šalje prvom autoru jedan primerak časopisa.

MVM *Editorial Board*
University of Kragujevac
Faculty of Engineering
Sestre Janjić 6, 34000 Kragujevac, Serbia
Tel.: +381/34/335990; Fax: + 381/34/333192
www.mvm.fink.rs